Thermal effects on geologic carbon storage

Victor Vilarrasa[1,2 *] and Jonny Rutqvist[3]

[1] Institute of Environmental Assessment and Water Research (IDAEA), Spanish National Research Council (CSIC), Jordi Girona 18-26, 08034 Barcelona, Spain

[2] Associated Unit: Hydrogeology Group (UPC-CSIC)

[3] Lawrence Berkeley National Laboratory (LBNL), 1 Cyclotron Rd, Berkeley, CA 94720, USA

[*] Corresponding author: victor.vilarrasa@upc.edu

ABSTRACT

One of the most promising ways to significantly reduce greenhouse gases emissions, while carbon-free energy sources are developed, is Carbon Capture and Storage (CCS). Non-isothermal effects play a major role in all stages of CCS. In this paper, we review the literature on thermal effects related to CCS, which is receiving an increasing interest as a result of the awareness that the comprehension of non-isothermal processes is crucial for a successful deployment of CCS projects. We start by reviewing CO_2 transport, which connects the regions where CO_2 is captured with suitable geostorage sites. The optimal conditions for CO_2 transport, both onshore (through pipelines) and offshore (through pipelines or ships), are such that CO_2 stays in liquid state. To minimize costs, CO_2 should ideally be injected at the wellhead in similar pressure and temperature conditions as it is delivered by transport. To optimize the injection conditions, coupled wellbore and reservoir simulators that solve the strongly non-linear problem of CO_2 pressure, temperature and density within the wellbore and non-isothermal two-phase flow within the storage formation have been developed. CO_2 in its way down the injection well heats up due to compression and friction at a lower rate than the geothermal gradient, and thus, reaches the storage formation at a lower temperature than that of the rock. Inside the storage formation, CO_2 injection induces temperature changes due to the advection of the cool injected CO_2, the Joule-Thomson cooling effect, endothermic water vaporization and exothermic CO_2 dissolution. These thermal effects lead to thermo-hydro-mechanical-chemical coupled processes with non-trivial interpretations. These coupled processes also play a relevant role in "Utilization" options that may provide an added value to the injected CO_2, such as Enhanced Oil Recovery (EOR), Enhanced Coal Bed Methane (ECBM) and geothermal energy extraction combined with CO_2 storage. If the injected CO_2 leaks through faults, the caprock or wellbores, strong cooling will occur due to the expansion

of CO_2 as pressure decreases with depth. Finally, we conclude by identifying research gaps and challenges of thermal effects related to CCS.

Keywords: CO_2 transport; injection schemes; CO_2 storage; thermo-hydro-mechanical-chemical couplings; induced microseismicity; caprock integrity; well integrity; CO_2 leakage

1. INTRODUCTION

Huge amounts of greenhouse gases, especially carbon dioxide (CO_2), are emitted to the atmosphere each year (around 36 Gt were emitted in 2014) as a result of burning fossil fuels for energy production (Le Quéré et al., 2016). These greenhouse gases retain the heat coming from the sun, which alters atmospheric circulations and therefore, the climate. To mitigate the negative effects of anthropogenic climate change, we should act quickly to significantly reduce these emissions. One of the most promising ways to reduce greenhouse gases emissions, at least in the short-term, while carbon-free energy sources are developed, is Carbon Capture and Storage (CCS) (IPCC, 2005). CCS consists in capturing CO_2 from the main point sources (e.g., steel and cement industries and coal and gas-fired power plants), transport the captured CO_2 to the injection wells and store it in deep geological formations.

CCS implies compression and expansion processes that cause pressure and temperature of CO_2 to vary over a wide range of values. During these variations, CO_2 may be present in gaseous, liquid or supercritical state. CO_2 properties, i.e., density, viscosity, specific heat capacity and enthalpy (Span and Wagner, 1996; Pruess and Garcia, 2002), as well as its solubility on water and brine (Duan and Sun, 2003; Harvey, 1996; Koschel et al., 2006) are strongly dependent on pressure and temperature. To reproduce these properties, the cubic equation of state of Redlich and Kwong (1949), with parameters adapted for CO_2 (Spycher et

al., 2003, 2005), is usually used for its simplicity and because good predictions are obtained (McPherson et al., 2008). Nevertheless, the equation of state of Span and Wagner (1996) is the most accurate one, but at the expenses of a high computational cost derived from the high complexity of its algorithm (Böttcher et al., 2012). Regardless of the equation of state that is considered, the strong dependency of CO_2 properties on pressure and temperature complicates the processes that occur in CCS.

Non-isothermal effects play a major role in all stages of CCS (Figure 1). However, to facilitate the understanding and solution of CCS processes, isothermal conditions have been usually considered. As a result, most of the knowledge gained on the processes involved in CCS neglects thermal effects. Nevertheless, the awareness that the comprehension of non-isothermal processes is crucial for a successful deployment of CCS projects has recently motivated an increasing interest to understand thermal effects.

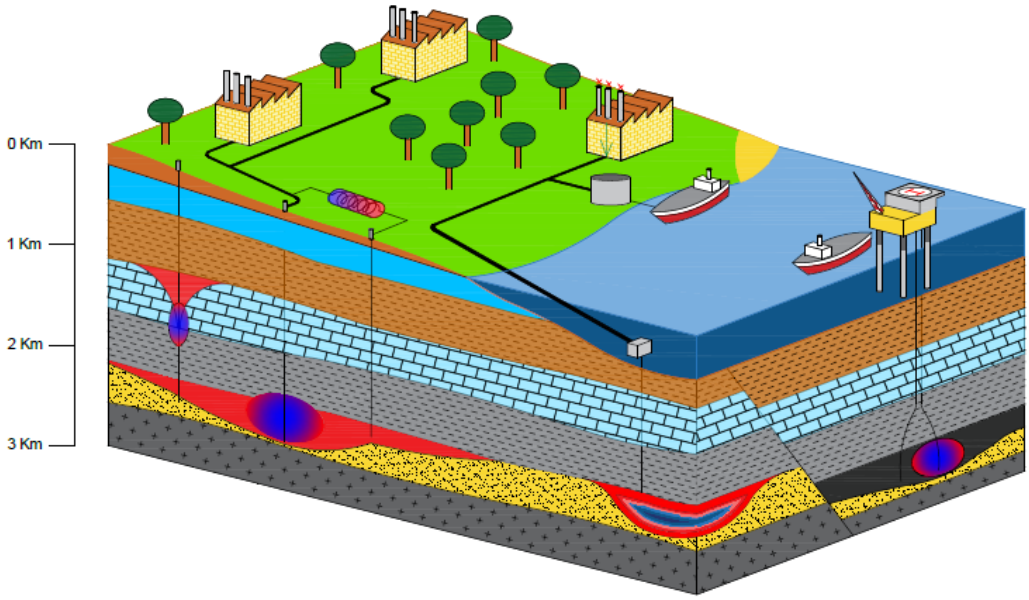

Figure 1. Schematic representation of thermal effects on CCS.

In this review, we present the state-of-the-art of the thermal effects related to CO_2 transport, injection, storage and leakage. First, we detail CO_2 transport both onshore and

offshore. Next, we present CO_2 injection options and how CO_2 properties change inside the injection well. Then, we focus on CO_2 storage in deep geological formations, looking at thermo-mechanical and thermo-chemical coupled processes and to options of utilization that provide an added value to the injected CO_2. Furthermore, we elaborate on potential CO_2 leakage through wells and faults. Finally, we conclude by identifying the existing research gaps and challenges related to thermal effects on geologic carbon storage.

2. CO_2 TRANSPORT

While CO_2 is mainly emitted onshore, both onshore and offshore geological formations may be suitable for storage. In general, CO_2 will have to be transported from the sources where it will be captured up to the storage sites. The optimum CO_2 transport options differ for onshore and offshore transportation. While for onshore transportation pipelines are the only feasible option (Svensson et al., 2004), both pipelines and ships can provide good solutions for offshore transportation. Though other options exist for onshore transportation, such as motor carriers and railways, they are not competitive because they are very expensive and of limited capacity (Skovholt, 1993). As for offshore transportation, ships are more flexible than pipelines, but require intermediate storage facilities, such as steel tanks or underground caverns, at harbors. On the other hand, pipelines require fewer logistics than ships and provide a continuous flow rate, but they imply building a new infrastructure on the seabed (Svensson et al., 2004).

Optimal marine transport conditions are obtained in semi-pressurized vessels of around 20,000 m^3 in liquid conditions close to the triple point, at 0.65 MPa and -52 ºC (Aspelund et al., 2006). These conditions yield CO_2 densities around 1,100 kg/m^3, which optimize the transport in terms of volume. The most expensive process for ship transport is the liquefaction and gas conditioning previous to filling the ships. But costs could be reduced by using the

liquid conditions of onshore pipelines when arriving at harbors for loading the ships. The efficiency of the system could be improved further by recovering CO_2 cold energy with a Rankine cycle during ship delivery, in which CO_2 has to be heated up to avoid injectivity issues due to ice or hydrate formation in the storage formation (You et al., 2014).

In pipelines, the best way to transport CO_2 is also in liquid state (McCoy and Rubin, 2008). Transport in gas phase is non-economical because of its low density, which requires large diameter pipes and implies high pressure drops. Pressure drop depends on the flow rate and the geometric characteristics of the pipe, i.e., diameter, length, elevation gain. Transport of supercritical CO_2 is preferable to transport of gaseous CO_2, but still, it induces a higher pressure drop than in liquid conditions, causing a decrease in density and thus, an increase in velocity, which, in turn, enhances the pressure drop. This enhanced pressure drop would lead to shorter distances between booster stations. Booster stations should be placed such that two-phase flow is avoided within the pipeline. Actually, operation of pipelines onshore may present difficulties in hilly terrain because pressure will decrease at the top of the hills, where CO_2 may turn into gas, giving rise to a two-phase flow, which is complicated to handle (Skovholt, 1993). Thus, transport of CO_2 is preferable in liquid state rather than in supercritical conditions due to the lower compressibility and higher density of liquid CO_2. Though liquid CO_2 has a higher viscosity than supercritical CO_2 (around 30%), CO_2 transport in liquid conditions permits using smaller pipe diameters, leading to lower pressure drops and thus, a more efficient transport (McCoy and Rubin, 2008; Nimtz et al., 2010).

To maintain liquid conditions, burying CO_2 pipelines can help controlling operation pressure and temperature conditions because underground temperature is more stable than surface temperature. In warm climates, where ground surface temperature can reach 65 ºC at noon, the temperature 1 m underground remains below 30 ºC (Zhang et al., 2006). Despite the higher installation costs derived from burying pipelines, the higher energy efficiency will

offset the initial investment because operation costs are around 15 % lower for liquid than for supercritical CO_2 transport (Zhang et al., 2006). Alternatively, in warm climates, insulating the pipeline and cooling the CO_2 to maintain liquid conditions may prove economical because of the lower pressure drop and therefore, lower number of booster stations for repressurizing CO_2 (Zhang et al., 2006). Furthermore, if CO_2 remains in liquid state, pumps, which are easier to operate than compressors, can be used to boost pressure. But apart from operational and economic reasons, pipelines will likely be buried for environmental, security and safety reasons.

CO_2 is not toxic, but it can be fatal if its concentration exceeds 10 % by volume because CO_2 produces asphyxia (Baxter et al., 1999). CO_2 could accumulate in depressions if there were a CO_2 leakage in a pipeline because CO_2 is heavier than air. Since CO_2 is colorless and odorless, humans and animals cannot detect CO_2 leakage and accumulation. Adding mercaptans, which people can easily identify because they are already added to natural gas, would be very beneficial because people could quickly react in case of CO_2 leakage (Gale and Davison, 2004). Nevertheless, an advisable practice would be to construct pipelines avoiding human settlements and to place CO_2 detectors along pipelines.

Other safety issues are related to the depressurization of a pipeline, either because it fails or due to planned maintenance. In such case, CO_2 will experience a phase change (from liquid to gas) which will cause a strong cooling. Such cooling should be taken into account in pipeline design to avoid brittle failure. This cooling may be limited by adding impurities to CO_2. For example, Munkejord et al. (2010) found that, for CO_2 mixtures with CH_4, the cooling due to evaporation becomes lower as the CO_2 content decreases. However, impurities may lead to enhanced pipe corrosion.

The construction of pipelines for CO_2 transport should be planned carefully because scale effects are relevant. For example, large diameter pipelines are much cheaper to operate than

several small pipelines with equivalent capacity. Thus, it is advisable to do a strategic planning to connect the source points where CO_2 will be captured with the storage regions using a single large pipeline, rather than several smaller pipelines. A significant experience with CO_2 pipelines exists in the USA, where an extensive CO_2 pipeline infrastructure (several thousands of km) already exists, mainly carrying naturally occurring CO_2 for enhanced oil recovery (EOR). These pipelines have proven to be safe in terms of potential for CO_2 release and thus, they do not represent a serious public hazard (Gale and Davison, 2004).

3. INJECTION OPTIONS

Since CO_2 will remain in supercritical conditions at the pressure and temperature conditions of storage formations, it is usually assumed that CO_2 will be injected in supercritical state. However, CO_2 needs to be transported from the source points, which are usually large industries or power plants, to the injection wells, which will likely be separated by several tens or even hundreds of km. CO_2 transport will be done through pipelines if it is onshore or through ships or pipelines if it is offshore. The optimum conditions for transporting CO_2 is in liquid conditions both for pipelines and ships (see Section 2). Thus, CO_2 will reach the wellhead in liquid state. For this reason, injecting in liquid state seems the most reasonable option.

Liquid CO_2 injection has some advantages. Silva et al. (2011), who proposed to inject CO_2 directly in liquid state, showed that liquid CO_2 injection is an energetically efficient injection concept. For the pressure and temperature ranges typical of injection wells, the density of liquid CO_2, which may reach values close to those of water density (in the order of 750 to 950 kg/m^3), is significantly higher than that of supercritical CO_2 (in the order of 250 to 700 kg/m^3) (Figure 2). Thus, just by gravity, liquid CO_2 flows downwards more easily, which implies that a lower compression energy is required to inject CO_2 (Vilarrasa et al., 2013). However, liquid

188 CO_2 injection has been feared because of its cold temperature, which induces thermal
189 contraction and associated stress reduction that may cause fracture instability in the storage
190 formation, the caprock, and/or the wellbore.

191 Thermal stresses induced by temperature difference between the wellbore and the
192 surrounding rock may lead to casing failure (Teodoriu, 2015). These stresses may become
193 large if the temperature change in the wellbore is large and fast (Kaldal et al., 2015).
194 Furthermore, if thermal cycling occurs as a result of alternating periods of CO_2 injection
195 (cooling) with shut-downs (heating), radial fractures or debonding of the cement may occur,
196 which could lead to CO_2 leakage (Roy et al., 2016). To minimize the risk of damaging the
197 cement, the use of non-shrinking cements is recommendable (McCulloch et al., 2003).

198 Apart from the cold temperature, the high pressure of liquid CO_2 has also been suspected
199 to potentially induce stability issues in the storage formation and caprock. Nimtz et al. (2010)
200 argued that liquid CO_2 might fracture the storage formation and caprock due to the high
201 overpressure that liquid injection would induce. However, Nimtz et al. (2010) did not couple
202 the pressure at the bottom of the injection well resulting from CO_2 injection along the
203 wellbore with the pressure at the injection well induced by CO_2 injection into the reservoir.
204 Actually, when coupling the wellbore simulator with the reservoir simulator, it has been
205 shown that the injection of 1 Mt/yr of CO_2 in a 100 m-thick reservoir with a permeability of
206 10^{-13} m^2 can be done maintaining liquid conditions along the wellbore and without inducing a
207 large overpressure in the reservoir (Vilarrasa et al., 2013). Thus, excessive overpressure is not
208 necessarily an issue of liquid CO_2 injection. Nevertheless, thermal effects may still be a
209 concern (see Section 5b). But to avoid cooling in the reservoir, and thus, inject in supercritical
210 conditions, CO_2 would need to be heated. At Ketzin, Germany, CO_2 was heated before
211 injecting it, leading to a temperature at the bottom of the injection well slightly higher than
212 that of the reservoir (Liebscher et al., 2013). The CO_2 injection rates at the pilot test site of

213 Ketzin were lower than 1 kg/s, so the energetic cost of heating was not excessive. However, at
214 industrial scale, heating would dramatically increase the energetic cost of injection in CO_2
215 storage projects (Möller et al., 2014; Goodarzi et al., 2015). Goodarzi et al. (2015) estimated
216 the cost of heating to avoid cooling the reservoir in 0.75 $\$/m^3$, which for an injection of 1
217 Mt/yr would represent a heating cost higher than 1 million dollars per year.

218 Pipelines can also be used for transporting CO_2 offshore. In this case, the pipeline lies on
219 the seabed and CO_2 thermally equilibrates with the seawater. Seawater is usually below the
220 CO_2 critical temperature, i.e., 31.04 ºC, and thus, liquid conditions will be easily maintained
221 within the pipeline. The transported liquid CO_2 will generally be injected directly into the
222 injection well, as happened at Snøhvit, Norway (Hansen et al., 2013). At Snøhvit, the water of
223 the North Sea is cold (about 4 ºC at the seabed), so the compression costs for injecting CO_2
224 are minimized because CO_2 has a high density at these temperatures.

225 When offshore transport is done through ships, CO_2 stays at -52 ºC. If CO_2 injection is
226 performed just by compressing CO_2 as it arrives in the ship, CO_2 would reach the storage
227 formation at a temperature well below that of hydrate formation (around 12 ºC) and freezing
228 (around 0 ºC) temperatures, which would block the pores surrounding the injection well
229 (Krogh et al., 2012). To heat up CO_2 before injection, seawater may be used (Aspelund et al.,
230 2006). However, using seawater to heat CO_2 implies losing energy that could otherwise be
231 recovered. For example, cold energy is already recovered from liquefied natural gas (Shi and
232 Che, 2009; Choi et al., 2013; Wang et al., 2013) and it can also be recovered for the cold CO_2
233 transported in ships. You et al. (2014) proposed to use a Rankine cycle between the CO_2
234 transported in ships and the injection conditions to produce electricity. They found that using
235 ammonia as the working fluid in the Rankine cycle yielded the best performance in terms of
236 power generation. The energy that can potentially be recovered in the heating process from
237 ship transport conditions to injection conditions is estimated to be $33.6 \cdot 10^6$ kWh for a mass

238 flow rate of 1 Mt/yr. The energy that could be effectively recovered by the Rankine cycle is
239 about $28.8 \cdot 10^6$ kWh for a mass flow rate of 1 Mt/yr (You et al., 2014), which is equivalent to
240 the mean electricity consumed by 5,780 people in the EU (Eurostat, 2016).
241

242 ## 4. CO_2 ALONG THE WELLBORE

243 When injecting CO_2 along the injection well, CO_2 exchanges heat with the surrounding
244 rock (Brill and Mukherjee, 1999). Not only does this heat exchange influence the CO_2 flow
245 pattern inside the well, but also the surrounding rocks and well components are affected by
246 CO_2-induced temperature changes. CO_2 is heated as it flows downwards because of
247 compression and frictional forces, but usually at a lower rate than that of the geothermal
248 gradient (Lu and Connell, 2008; Luo and Bryant, 2010). Thus, CO_2 within the well is, in
249 general, colder than the rock, especially at high flow rates (Paterson et al., 2008; 2010). For
250 example, the CO_2 temperature at the bottom of the injection well at Cranfield, Mississippi,
251 increased by 16 ºC when the mass flow rate was reduced by a factor of 4 (Luo et al., 2013),
252 showing that high flow rates of injection lead to lower injection temperatures. Another
253 representative example is the CO_2 injection at In Salah, Algeria, where CO_2 temperature at the
254 wellhead coincided with that of the surface temperature, but CO_2 reached the storage
255 formation at 1800 m deep 45 ºC colder than the temperature corresponding to the geothermal
256 gradient (Bissell et al., 2011).

257 The lower temperature of CO_2 cools down the rock surrounding the well. But the heat
258 exchange between CO_2 and the surrounding rock is usually limited in time when a constant
259 mass flow rate is injected and thermal equilibrium may be reached within hours or a few days
260 (Lu and Connell, 2008). Once thermal equilibrium between CO_2 and the surrounding rock is
261 reached, adiabatic conditions occur within the injection well. Transient effects are sometimes
262 neglected to simplify calculation (Nimtz et al., 2010). However, heat exchange cannot be

neglected in the case of blowouts (Lindeberg, 2011) or if CO_2 injection is not continuous (Lu and Connell, 2014a).

Current wellbore simulators, e.g., T2Well (Pan and Oldenburg, 2014), are capable of handling transient effects. For instance, Lu and Connell (2014a) developed a transient non-isothermal wellbore flow model for multispecies mixtures. Lu and Connell (2014a) found that steady heat transfer models might be inappropriate for unsteady flows. Previous models based on steady or quasi-steady flow models (e.g., Lu and Connell, 2008), partly or fully neglected the effects of storage and inertial terms in the flow equations. This quasi-steady approach is acceptable for injections of months or years, but not for unsteady conditions, e.g., non-uniform flow rate. Lu and Connell (2014a) presented an example of Enhanced Coal Bed Methane (ECBM). ECBM is a method to produce methane from coal beds by injecting CO_2, which adsorbs in the coal, displacing methane. Lu and Connell (2014a) obtained a good fitting of pressure and temperature at both the wellhead and bottomhole. CO_2 was injected in liquid conditions from a tanker truck (at around 1.5 MPa and -30 ºC, very close to the saturation line), and two-phase flow conditions took place within the first meters of the well due to partial vaporization of the liquid CO_2.

Another field test of CO_2 injection for ECBM purposes was carried out at Yuhbari, Hokkaido, Japan, between 2003 and 2007 (Sasaki et al., 2009). The coal seam was at 900 m deep, with a pressure and temperature of approximately 15.5 MPa and 28 ºC, respectively. Sasaki et al. (2009) found that coal permeability decreased up to a factor of 15 as the coal became saturated in CO_2 due to swelling of coal. However, this swelling effect decreased for successive injection experiments. Furthermore, the intrinsic permeability around the injection well increased for successive injection experiments up to a factor of 6 due to fracturing of the rock. CO_2 was injected at 68.5 ºC, but CO_2 reached the bottom of the injection well in liquid conditions, i.e., below 31.04 ºC, due to heat loss along the injection well. The reason for such

288 high injection temperature was the intention to inject CO_2 in supercritical conditions rather
289 than in liquid state because the lower viscosity of supercritical CO_2 would facilitate CO_2
290 injection in such a low permeable formation. However, even insulating the injection tubing
291 was not enough to increase CO_2 temperature at low flow rates (4.5 ton/day). It was estimated
292 that to achieve supercritical conditions at the bottom of the injection well, a flow rate higher
293 than 12 t/day, i.e., 0.14 kg/s or 4380 t/yr, would be necessary.

294 These examples illustrate that pressure, temperature and density profiles along the wellbore
295 can be complex (Figure 2) and significantly vary for small changes in the pressure and
296 temperature at the wellhead (Vilarrasa et al., 2013). Since density depends on both pressure
297 and temperature, the system is strongly coupled and the CO_2 flow along the wellbore is not
298 trivial. This complexity is especially true when the injection conditions at the wellhead are
299 close to phase change (Lu and Connell, 2014b). For example, at Ketzin, Germany, CO_2 was
300 initially in gas state in the shallower 100 m of the well and in liquid state in the rest, but after
301 a transient period, two-phase flow conditions extended practically all along the well
302 (Henninges et al., 2011). Another example is that of Sleipner, Norway, where two-phase (gas
303 and liquid CO_2) conditions exist at the wellhead, the two-phase flow is maintained for the first
304 250 m of the injection well, but the phase that remains below the two-phase region can be
305 liquid instead of gas for slight changes in the wellhead conditions (Lindeberg, 2011).

306 To complicate the process even further, the pressure, temperature and density variation
307 with depth along the wellbore is also controlled by the overpressure induced at the storage
308 formation for a given flow rate. Thus, the resulting pressure and temperature conditions at the
309 wellhead will also depend on the injectivity of the storage formation. Therefore, wellbore
310 simulators should be coupled with reservoir simulators to properly model the CO_2 pressure
311 and temperature, which determines the density, along the injection well (Pan et al., 2011; Pan
312 and Oldenburg, 2014; Vilarrasa et al., 2013).

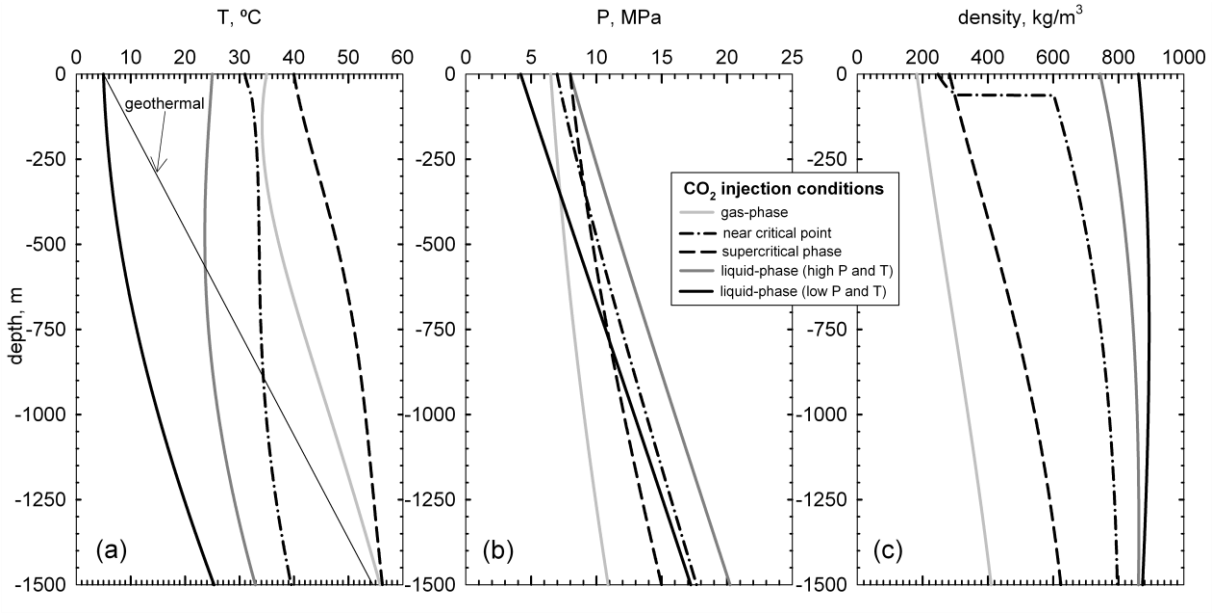

Figure 2. Non-isothermal flow of CO_2 through an injection well: temperature (a), pressure (b) and density (c) profiles. Comparison between different injection conditions at the wellhead (gas-, supercritical- and liquid-phase) (injection rate of 1.5 kg/s, geothermal gradient of 0.033 ºC/m, well radius of 4.5 cm, overall heat transfer coefficient of 10 W m^{-2} K^{-1}) (from Vilarrasa et al.,2013).

5. CO_2 STORAGE

a. CO_2 INJECTION IN DEEP SEDIMENTARY FORMATIONS

CO_2 injection in deep saline formations induces temperature changes owing to processes such as Joule-Thomson cooling, endothermic water vaporization, exothermic CO_2 dissolution (Han et al., 2010; 2012) and because CO_2 will, most likely, reach the storage formation at a colder temperature than that corresponding to the geothermal gradient (Vilarrasa et al., 2014). When CO_2 enters into the storage formation, temperature slightly drops, by some decimals of degree, in the first tens of meters around the injection well, due to Joule-Thomson cooling as pressure drops with distance to the well (Han et al., 2010). The Joule-Thomson cooling effect may be more pronounced in depleted oil and gas fields due to the expansion of CO_2 when it

enters into the low pressure reservoir (Oldenburg, 2007; Pekot et al., 2011; Singh et al., 2011a). However, the induced cooling is unlikely to cause injectivity problems due to hydrate formation that could clog the well, except for initially cold reservoirs (T<20 ºC) (Mathias et al., 2010; Ding and Liu, 2014). Apart from the Joule-Thomson cooling effect, water vaporization into the dry CO_2 causes an additional cooling of around 1.0-2.0 ºC. Water vaporization only occurs in the vicinity of the injection well, within the first tens of meters in the radial distance, because further away CO_2 becomes saturated with water. Outside the vaporization front, temperature rises due to the exothermic CO_2 dissolution into the brine (André et al., 2010; Han et al., 2010). The temperature increase due to CO_2 dissolution is of around half degree and may be used for monitoring the advancement of the CO_2 plume (Bielinski et al., 2008; Zhao and Cheng, 2014). Actually, a visible temperature signal can be detectable upon CO_2 arrival at an observation well in the storage formation, as occurred at the CO_2 injection pilot test sites of Frio, Texas (Hovorka et al., 2006) and Nagaoka, Japan (Sato et al., 2009).

The dynamics of the CO_2 plume is governed, in part, by CO_2 density. While high CO_2 density leads to a viscous dominated flow, low CO_2 density yields gravity dominated CO_2 flow. CO_2 density depends on both pressure and temperature, which are not straightforward to determine within the CO_2 plume, as shown by the existing uncertainty on the actual CO_2 density of the CO_2 plume at Sleipner, Norway (Nooner et al., 2007; Alnes et al., 2011). Initially, pressure may be hydrostatic and predictable, but it may also vary significantly, such as in depleted petroleum reservoirs. During CO_2 injection, an overpressure that is inversely proportional to permeability is induced and thus, CO_2 density will increase with injection. However, the range of CO_2 density change due to overpressure is limited, in general, to some tens of kg/m^3 (Figure 3). The geothermal gradient is also site dependent, which, for the depths of storage, i.e., several km, may give rise to temperature variations of tens of degrees between

different storage sites (Randolph and Saar, 2011b). As a result, CO_2 density can vary several hundreds of kg/m^3 from a storage site placed in a sedimentary basin with a high geothermal gradient to a site with a low geothermal gradient (Bachu, 2003) (Figure 3). The warmer the storage formation, the lower the CO_2 viscosity, which will facilitate flow and decrease overpressure (Wiese et al., 2010), but may enhance viscous fingering (Jackson et al., 2015). Temperature also affects the surface tension and the wetting angle, which play a role in capillarity (Singh et al., 2011b). The occurrence of these processes implies that it is important to account for non-isothermal effects even though CO_2 is injected in thermal equilibrium with the storage formation (Class et al., 2009).

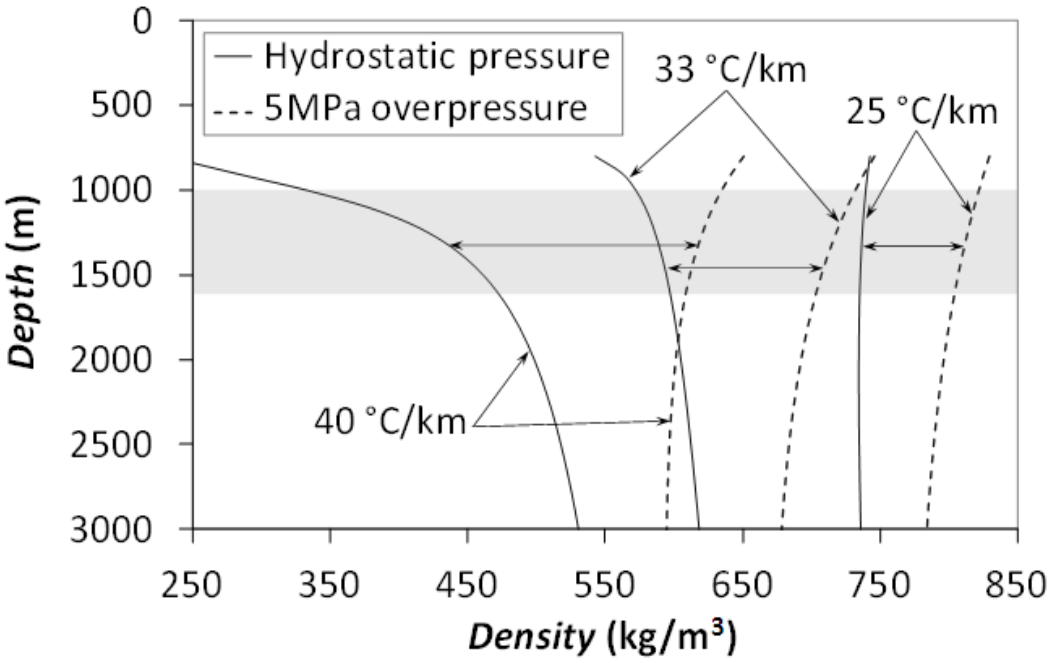

Figure 3. CO_2 density as a function of depth for several geothermal gradients at hydrostatic conditions and for a 5 MPa overpressure generated by CO_2 injection. Surface temperature is of 5, 10 and 15 ºC for the geothermal gradients of 25, 33 and 40 ºC/km, respectively. The shadowed region is the most appropriate depth interval for geologic carbon storage because it is deep enough to ensure a high CO_2 density that permits an efficient storage in terms of

volume, and also because deeper storage formations would imply higher drilling and injection costs.

Thermal effects are more evident when the injected CO_2 is colder than the storage formation. In such case, CO_2 cools down the rock around the wellbore, forming a cooler region that tends to reach the same temperature as that of the inflowing CO_2 (Vilarrasa et al., 2013). This cold region advances much behind of the desaturation front because CO_2 is heated by the rock, which retards the advance of the cooling front with respect to the front of the CO_2 plume. The colder CO_2 is denser and more viscous than the supercritical CO_2 that is in thermal equilibrium with the storage formation. Thus, viscous forces dominate in the cooled region, leading to a steep CO_2 front that sweeps most of the thickness of the storage formation (Rayward-Smith and Woods, 2011). However, as CO_2 warms up, its lower density and viscosity leads to gravity override and thus, CO_2 tends to advance through the top portion of the storage formation (Vilarrasa et al., 2014). The denser CO_2 in the cooled region occupies a smaller volume than supercritical CO_2 and thus, displaces a smaller amount of brine, which results in a slightly lower overpressure for cold CO_2 injection than for CO_2 in thermal equilibrium with the storage formation (Vilarrasa et al., 2013; Randolph et al., 2013; Zhao and Cheng, 2015). Furthermore, the cold region around the injection well remains for a long period of time after the end of injection because the cooling front advances mainly by advection of the cold CO_2 during injection, but the cooled rock is heated up by heat conduction afterwards, which leads to a period to reach thermal equilibrium that is longer than the injection period.

b. **THERMO-MECHANICAL EFFECTS**

CO_2 injection in deep saline formations implies temperature changes that will induce stress and strain (Rutqvist, 2012). The region undergoing the largest temperature change will be limited to a few hundreds of meters from the injection well for a CO_2 injection of several decades. This region is relatively small compared to the extent of the CO_2 plume, which may reach several kilometers (Vilarrasa et al., 2014). Still, thermal stresses may be a concern (Celia et al., 2015) because CO_2 will, in general, reach the storage formation colder than the rock, which may bring the stress state closer to failure conditions (de Simone et al., 2013). Major faults will rarely be cooled down because injection wells will be placed far from them. However, the thermal contraction of the rock around the injection well affects the stress field in the far-field through deformations and associated stress-transfer and thus, the stability of faults placed far away from the well may be reduced (Jeanne et al., 2014). This contraction of the rock caused by cooling also leads to a smaller surface uplift induced by cold CO_2 injection compared to CO_2 injection in thermal equilibrium with the storage formation (Goodarzi et al., 2012; Fang et al., 2013). Furthermore, the lower portion of the caprock in the vicinity of injection wells will be cooled down due to heat conduction once the cold CO_2 reaches the top of the storage formation. This cooling may induce fracture instability within the caprock, especially if the thermal expansion coefficients of the two formations are different (Vilarrasa and Laloui, 2016).

Shear slip of fractures within the caprock and hydraulic fracture formation and propagation across the caprock is, in principle, undesirable. However, in the presence of thick caprocks, the overall caprock sealing capacity may not be compromised even though shear or tensile failure conditions are reached at the bottom of the caprock, as demonstrated at In Salah, Algeria. At this site, no leakage has occurred in spite of the fact that cooling probably contributed to induce shear failure of the lower portion of the caprock (Vilarrasa et al., 2015).

419 Nevertheless, it is important to minimize the disturbance of the caprock integrity (Sagu and
420 Pao, 2013). Thus, thermal stresses should be accounted for to determine the maximum
421 sustainable injection pressure and maximum temperature drop that can be induced without
422 compromising the caprock integrity (Rutqvist et al., 2011; Kim and Hosseini, 2014b, 2015).
423 The distribution of thermal stresses is controlled by the extension of the cold region.
424 Analytical (Bao et al., 2014) and semi-analytical (LaForce et al., 2015) solutions have been
425 developed to estimate the position of the cold region and the induced thermal stresses. Even
426 though good estimates are obtained at the beginning of injection, when viscous forces
427 dominate and the CO_2 plume advances as a plug, differences arise as CO_2 moves away from
428 the injection well and gravity forces dominate, which leads to a cooling front that
429 preferentially advances along the top of the storage formation. Better estimates can be
430 obtained for the injection of brine with dissolved CO_2 because buoyancy forces are much
431 smaller than when a CO_2-rich phase is injected (Wu and Bryant, 2014). Nevertheless, this
432 thermo-hydro-mechanical coupled problem should be solved numerically to obtain accurate
433 solutions.
434 Numerical results are used to predict cooling-mediated hydraulic fracture initialization,
435 which occurs when the minimum effective stress exceeds the tensile strength of the rock
436 (Goodarzi et al., 2011, 2013; Luo and Bryant, 2011, 2013; Taylor and Bryant, 2014).
437 Hydraulic fractures, or shear slip of pre-existing fractures, may be beneficial if they are
438 confined within the storage formation because injectivity is enhanced (Goodarzi et al., 2010;
439 Rutqvist, 2012). Luo and Bryant (2014) modeled fracture propagation due to cooling in the
440 storage formation and found that stiff storage formations experience fast fracture growth,
441 leading to a low usage efficiency of the storage formation because the CO_2 plume becomes
442 elliptical as CO_2 advances preferentially along the hydraulic fracture. In contrast, soft storage
443 formations yield slow fracture propagation that may stop close to the well, giving rise to a

444 cylindrically-shaped CO_2 plume with high usage efficiency of the storage formation. Thus,
445 using thermal stresses properly can contribute to enhance the injectivity in the storage
446 formation. However, the propagation of hydraulic fractures or shear slip of pre-existing
447 fractures from the storage formation into the caprock should be avoided or, at least,
448 minimized to maintain the caprock sealing capacity. Apart from the magnitude of each stress
449 component and overpressure (Goodarzi et al., 2012; 2015), the propagation of shear or tensile
450 failure conditions from the storage formation into the caprock is controlled by several factors,
451 such as the stress regime, stress and strength heterogeneity between layers and the distance
452 from the injection well to the caprock.

453 Regarding the stress regime, strike slip stress regimes (i.e., stress states in which the
454 vertical stress is the intermediate principal stress) are more likely to propagate failure
455 conditions into the caprock than normal faulting (i.e., when the vertical stress is the maximum
456 principal stress) and reverse faulting stress regimes (i.e., when the vertical stress is the
457 minimum principal stress) (Vilarrasa, 2016). For example, simulation results of cold CO_2
458 injection at In Salah, Algeria, which is characterized by a strike slip stress regime, show that
459 the lower part of the caprock is likely to reach shear and tensile failure conditions (Preisig and
460 Prevost, 2011; Gor and Prévost, 2013; Gor et al., 2013; Vilarrasa et al., 2015). However, in
461 normal faulting stress regimes, failure conditions may not occur into the caprock even though
462 shear failure conditions are reached within the storage formation (Vilarrasa and Laloui, 2015).
463 This is because cooling of the storage formation induces a thermal stress reduction in all
464 directions, but since the overburden on top of the storage formation remains constant, a local
465 discontinuity in the vertical stress between the storage formation and the caprock appears
466 around the injection well. Therefore, stress redistribution occurs around the cooled region to
467 satisfy stress equilibrium and displacement compatibility. This stress redistribution causes the
468 horizontal total stresses of the lower portion of the caprock to increase, similar to an arch

effect, around the cooled region. The higher horizontal stresses tighten the caprock in a normal faulting stress regime, improving its stability (Vilarrasa et al., 2013). A similar stress redistribution occurs in a reverse faulting stress regime, but in this case, since the maximum principal stress is horizontal, the deviatoric stress increases in the caprock. However, due to the high confinement pressure, the decrease in stability is small, so fracture propagation across the caprock is unlikely. Only the caprock-reservoir and baserock-reservoir interfaces may reach failure conditions, but without propagating into the caprock (Bao et al., 2014). Furthermore, the stability within the storage formation may improve due to cooling in a reverse faulting stress regime, because, in the long-term, the horizontal stresses undergo a larger thermal stress reduction than the vertical stress, which decreases the deviatoric stress (Vilarrasa et al., 2014) (see Table 1 for a summary of the stress regime on rock stability changes induced by cooling).

Table 1. Thermo-mechanical effects of cooling on rock stability as a function of the stress regime

Stress regime	Storage formation	Caprock
Normal Faulting	Thermal stress reduction in both the maximum and the minimum	Stress redistribution around the cooled region increases the minimum (horizontal) principal stress, reducing the deviatoric stress, which tightens the caprock

Strike Slip	principal stresses brings the stress state closer to failure conditions	Stress redistribution around the cooled region affects equally the maximum (horizontal) and the minimum (horizontal) principal stresses, so the thermal stress reduction shifts the stress state closer to failure conditions maintaining the deviatoric stress
Reverse faulting		Stress redistribution around the cooled region increases the maximum (horizontal) principal stress, which increases the deviatoric stress, but just slightly due to the high confining stress

As far as the stress anisotropy between layers is concerned, caprocks are usually softer than storage formations and thus, caprocks tend to accumulate less deviatoric stress than storage formations as a result of tectonic plate movements (Hergert et al., 2015). This stress heterogeneity between the storage formation and the caprock makes fracture propagation into the caprock less likely. For example, Goodarzi et al. (2015) modeled the Ohio River Valley, West Virginia, which is a strike slip stress regime, and therefore, thermal stresses are likely to induce fracture propagation into the caprock, as may have occurred at In Salah, Algeria (Gor et al., 2013; White et al., 2014). However, when accounting for the stress heterogeneity between geological layers, hydraulic fractures may not propagate into the caprock because of its higher minimum effective stress in normal faulting and strike slip stress regimes. Furthermore, unlike in the storage formation, shear failure conditions may not be reached in the caprock due to the lower deviatoric stress.

As for the position of the injection well with respect to the caprock, placing the well away from the caprock may help to avoid inducing large thermal stresses in the caprock (Vilarrasa et al., 2014). For example, Bonneville et al. (2014) used a 3D model with 4 horizontal wells to simulate the CO_2 pilot site of FutureGen 2.0, Illinois. Tensile stresses were predicted at some points close to the injection well when CO_2 was injected colder than the storage formation. However, the top of the storage formation remained in compression because the cooling front did not reach it during the simulation time. Nevertheless, the cooling front is likely to eventually reach the caprock due to the buoyancy of CO_2. Yet, if the injection well is placed at a certain distance from the caprock, the temperature drop will be smaller than at the injection well, as occurred at Cranfield, Mississippi (Kim and Hosseini, 2014a; Luo et al., 2013).

c. THERMO-GEOCHEMICAL PROCESSES

One issue related to CO_2 injection in deep saline formations is salt precipitation around the injection well (Pruess and Garcia, 2002). CO_2 will form a CO_2-rich region around the injection well where liquid saturation will be reduced to the residual liquid saturation. CO_2 will be preferably injected dry, because if water is present, corrosion problems in pipes are likely to occur. Thus, the residual brine will tend to evaporate into the dry CO_2, increasing the salt concentration in the liquid phase (André et al., 2011). Once the equilibrium solubility is reached, salt will precipitate, inducing crystallization pressure that might fracture the rock and open new percolation pathways if stresses become high enough (Osselin et al., 2013). Salt precipitation slightly decreases porosity. But since salt precipitates close to the pore throats, the connectivity between the pores may clog, which could cause a dramatic decrease in permeability and thus, in injectivity. Water evaporation increases at higher temperature (Spycher and Pruess, 2005). Thus, a higher temperature generally results in more salt

precipitation (Kim et al., 2012). However, as brine is evaporated, the relative permeability to CO_2 increases, which may partly compensate the permeability reduction due to salt precipitation (Mathias et al., 2011).

Apart from salt precipitation, temperature affects the reaction rates of chemical reactions (Song and Zhang, 2012). Geochemical reactions are more significant in carbonate rocks than in siliciclastic rocks because carbonate minerals tend to dissolve in response to CO_2 dissolution into the brine, which gives rise to an acidic solution. The solubility of both CO_2 and carbonate rocks is higher at lower temperature. Thus, more CO_2 dissolution and carbonate (mainly calcite and dolomite) dissolution will occur within the cold region that forms around the injection well due to cold CO_2 injection. However, cooling has a minor effect on the increment of the mineral volume fraction that is dissolved compared with CO_2 injection in thermal equilibrium with the storage formation (Tutolo et al., 2015). The porosity development around the injection well, which is the zone with the largest geochemical changes, is small due to the low solubility of calcite (Saaltink et al., 2013). Thus, formation of large cavities due to mineral dissolution should not be feared. If the temperature of the storage formation is higher than 60 ºC, dolomite precipitation is likely to occur, which may decrease porosity and permeability. Consequently, cold CO_2 injection may inhibit precipitation of carbonate minerals around the well in warm (>60 ºC) storage formations and thus, injectivity would not be negatively affected (André et al., 2010).

Geochemical reactions will lead to CO_2 mineral sequestration if carbon is fixed as carbonate minerals. Carbon mineralization permits a permanent storage of CO_2 with negligible leakage risk (Zevenhoven et al., 2011). This process is expected to occur in the time scale of hundreds to thousands of years in deep saline aquifers (Zhang et al., 2009). However, the mineralization process into carbonates can be dramatically speeded up in basaltic rocks, with a 95 % mineralization of the injected CO_2 in less than 2 years (Matter et

546 al., 2016). Mineralization of CO_2 may also be achieved in industrial processes, such as steel
547 and iron-making slags. These chemical reactions release significant amounts of heat, which
548 could be useful in some industrial processes and affect reaction rates in geomaterials
549 (Zevenhoven et al., 2011).
550
551 d. **CARBON CAPTURE, UTILIZATION AND STORAGE**
552 Recently, it has been argued that CO_2 injection in deep saline aquifers should be
553 accompanied by its "utilization" to provide an added value that makes CCS an economically
554 feasible option for reducing CO_2 emissions to the atmosphere. Thus, CCS should evolve to
555 Carbon Capture, Utilization and Storage (CCUS). One of the most feasible options is
556 Enhanced Oil Recovery (EOR), which consists in injecting CO_2 in mature oil fields to
557 enhance their productivity (Brown et al., 2004; Hill et al., 2013). CO_2 is miscible in oil and
558 reduces oil viscosity, facilitating oil production. However, most of the injected CO_2 returns to
559 the surface dissolved into the produced oil. At surface, CO_2 is forced to exsolve from oil and
560 is reinjected. If more CO_2 is injected than produced, as it has been done at Weyburn, Canada,
561 since 2004 (Verdon et al., 2011), CO_2 storage takes place. Similarly, CO_2 can be used for
562 Enhanced Gas Recovery (EGR) in depleted gas fields, where the Joule-Thomson cooling
563 effect may be significant (Singh et al., 2012).
564 CO_2 can be stored in unminable coal seams, in which CO_2 displaces the methane originally
565 adsorbed to coal, leading to ECBM production (White et al., 2005). This CCUS option relies
566 on the higher affinity of CO_2 than methane to adsorb to coal. The potential storage capacity of
567 ECBM, though lower than that of saline aquifers, is large (Gale, 2004). The main limitation of
568 ECBM may be the relatively low permeability of coal seams. To overcome this drawback,
569 CO_2 may be injected quite warm, so that its viscosity is low and thus, overpressure does not
570 become large (Sasaki et al., 2009).

571 Other alternative CCUS options focus on using the geothermal energy of the deep
572 geological formations where CO_2 will be stored. One of the CO_2 storage methods that
573 involves geothermal energy recovery is the injection of CO_2 dissolved into brine (Pool et al.,
574 2013). Since brine with dissolved CO_2 is denser than brine without dissolved CO_2, CO_2-rich
575 brine tends to sink towards the bottom of the storage formation, making long-term CO_2
576 storage safe, especially in sloping aquifers. This storage concept has the drawback that brine
577 needs to be pumped and afterwards re-injected together with CO_2, which increases drilling
578 costs and pumping/compression costs. However, these additional costs may be offset by
579 recovering the geothermal energy of the pumped brine, which has a temperature higher than
580 that at the surface (Pool et al., 2013; Kervévan et al., 2014).
581 Another method for recovering geothermal energy consists in using CO_2 as the working
582 fluid (Randolph and Saar, 2011a). The thermosiphon concept using CO_2 as a circulating fluid
583 in heat pipes (Ochsner, 2008) was adopted as a means of geothermal energy, partly storing
584 CO_2, in deep geological formations (Freifeld et al., 2013; Buscheck et al., 2013; Adams et al.,
585 2014). Interestingly, CO_2 will circulate in the thermosiphon without the need of pumping (Pan
586 et al., 2015). Cold CO_2, and therefore dense, is injected in liquid conditions through a well
587 into a deep geologic formation. CO_2 will warm up as it moves away from the injection well,
588 becoming supercritical CO_2, and thus lighter (Vilarrasa et al., 2013). This supercritical CO_2
589 will flow upwards due to buoyancy through another well, returning to the surface, where it
590 will release its heat and electricity will be produced (Elliot et al., 2013). Apart from
591 minimizing the energy required for injection and pumping, CO_2 is more efficient than water
592 as a circulating fluid and yields higher power production (Adams et al., 2015). Once
593 electricity has been produced and the heat of CO_2 utilized, CO_2 cools down. Then, the cold
594 CO_2 is injected again into the injection well. Thus, the use of CO_2, instead of water, as the
595 working fluid, allows making use of geothermal energy without the need of mechanical

pumping. Furthermore, most of the injected CO_2 will remain deep underground, where it will be permanently stored, and the economic benefit provided by the geothermal energy will convert geologic carbon storage into a feasible option to mitigate climate change.

6. CO_2 LEAKAGE THROUGH WELLS AND FAULTS

CO_2 leakage is a concern in geologic carbon storage because: (i) the objective of keeping CO_2 away from the atmosphere is not achieved (Hepple and Benson, 2005); (ii) freshwater aquifers may undergo acidification and contamination (Lu et al., 2010; Trautz et al., 2012; Ardelan and Steinnes, 2010); and (iii) asphyxiation hazard exists if CO_2 accumulates in depressions on the land surface. CO_2 may leak from the storage formation across the caprock, through faults or along wells. CO_2 leakage may be accompanied by brine leakage, which could also be a concern if it reaches freshwater aquifers (Tillner et al., 2013). To prevent both salinization of freshwater aquifers and CO_2 leakage from reaching the surface, multibarrier systems, where saline aquifers alternate with low-permeability formations that serve as caprocks, are an effective option (Birkholzer et al., 2009).

Natural analogues can provide useful information on the mechanisms that may promote CO_2 leakage. Miocic et al. (2014) analyzed 49 natural CO_2 reservoirs, 10 of which were known to leak. They found that leakage occurred either in shallow reservoirs, i.e., depths shallower than 1000 m, where CO_2 was in gaseous phase, or in pressurized reservoirs where the fracture gradient had been reached. The fact that reservoirs with gaseous CO_2 are more prone to leak than reservoirs containing supercritical CO_2 is probably due to the higher buoyancy of the less dense gaseous CO_2. On the other hand, reservoirs that are underpressurized with respect to the overburden are less likely to leak than reservoirs that are overpressurized with respect to the overburden. However, in geologic carbon storage, this factor will generally not be favorable due to the overpressure induced by CO_2 injection.

Though it has been proposed by Réveillère and Rohmer (2011) and Réveillère et al. (2012) to inject brine into the caprock to create a hydraulic barrier against CO_2 leakage, this injection could jeopardize the caprock integrity because fluid injection in the caprock would significantly increase pore pressure due to the low-permeability of the caprock. This pressure buildup would reduce the effective stresses and failure conditions could be reached, which could cause the opposite effect as the pursued one.

Unlike caprocks, which are likely to remain stable (Vilarrasa and Carrera, 2015), wellbores are the most likely conduit for CO_2 to escape from the storage formation, especially in sedimentary basins where hydrocarbons have been produced. A clear example of the potential effect of wellbores in hydrocarbon basins on CO_2 leakage is the Alberta Basin, Canada, which has more than 300,000 wells in 900,000 km^2 (Gasda et al., 2004). Some of the wellbore simulators used for calculating CO_2 injection along the injection well (recall Section 4) can also be used for calculating non-isothermal CO_2 leakage just by adding a few modifications (Pan et al., 2011; Pan and Oldenburg, 2014). Furthermore, some efforts have been made to explain CO_2 leakage through wells analytically (e.g., Nordbotten et al., 2004, 2005). However, the thermal effects that occur during CO_2 leakage make it very complicated to develop analytical or semi-analytical solutions that give good estimates of CO_2 leakage along abandoned wells. To illustrate this, Ebigbo et al. (2007) compared the semi-analytical solutions of Nordbotten et al. (2004, 2005) for leaky wells with numerical solutions. Ebigbo et al. (2007) found that the semi-analytical solutions compare well with the numerical simulations when the simplifying assumptions of the semi-analytical solution, which include isothermal conditions, are taken into account in the numerical model. However, as the simplifying assumptions are relaxed, numerical results increasingly differ from those of the semi-analytical solution. In particular, the semi-analytical solution fails to give good results when non-isothermal effects occur. This limitation was revealed by a model in which CO_2

changes from liquid to gas inside of a leaky well that connects two aquifers between 800 and 640 m deep, which gives rise to a 1.5 ºC drop at the top of the leaky well (depth of 640 m) due to the phase change.

The CO_2 dynamics in a leaky well can be very diverse. Initially, the wellbore is saturated with water. Once CO_2 starts leaking, water is initially displaced upwards due to the buoyancy of CO_2. As CO_2 advances upwards, CO_2 saturation increases due to gas exsolution as pressure decreases at shallower depths and, due to the lower density of gaseous than supercritical CO_2 (Pan et al., 2009). This phase change occurs when the pressure becomes lower than the critical CO_2 pressure of 7.4 MPa, i.e., at depths lower than about 800 m. If the amount of available CO_2 for leaking into the well is unlimited, a quasi-steady state is rapidly reached, within 30 minutes (Pan et al., 2011). The temperature profile stabilizes when the steady state flow is reached. But before this stabilization occurs, the temperature profile along the well reaches a maximum due to CO_2 dissolution into the water, which is an exothermic reaction, followed by a local minimum caused by CO_2 expansion. However, in general, CO_2 mobility in the reservoir controls the leakage rate through an open borehole and therefore, CO_2 availability will usually be limited. In particular, if the CO_2 saturation is close to the residual gas saturation, CO_2 cannot continuously flow through the wellbore, leading to a geyser like leakage (Pan et al., 2011). Furthermore, in closed reservoirs, CO_2 leakage induces a reduction of the reservoir pressure, which causes a progressive reduction of CO_2 leakage rate.

In the scenarios modeled by Pan et al. (2009; 2011), CO_2 transitioned from supercritical to gas without undergoing any phase change. This may be the case in the presence of high geothermal gradient. However, liquid CO_2 may appear due to the cooling that occurs during expansion when considering a broader range of geothermal gradients or for insulated wells that receive very limited heat from the surrounding rock (Oldenburg et al., 2012). Long-term CO_2 leakage may also lead to a similar situation than that of an insulated well once the

671 surrounding rock is cooled down and provides a low amount of heat to CO_2. If liquid CO_2
672 forms, the saturation line is eventually reached at a certain depth, where liquid and gas will
673 coexist. The depth interval where liquid and gas CO_2 coexist experiences strong non-
674 isothermal effects due to the Joule-Thomson effect (Burnett, 1923; Charnley et al., 1955) that
675 occurs as a result of the expansion that takes place when liquid CO_2 boils into subcritical
676 gaseous CO_2 (Pruess, 2011). This cooling results in an advance, mainly upwards, of the depth
677 interval where CO_2 stays on the saturation line (Oldenburg et al., 2012). Thus, the temperature
678 difference (cooling) with respect to the geothermal gradient becomes larger as the two-phase
679 conditions advance upwards. In extreme cases, CO_2 release in wells may lead to pressure and
680 temperatures at the wellhead close to those of the triple point (i.e., 0.511 MPa and -56.35 ºC,
681 respectively). If such conditions are reached, CO_2 will be ejected as solid "dry ice" particles,
682 as has already occurred in EOR fields (Skinner, 2003). Similar processes would occur if CO_2
683 leakage occurs through a fault instead than through a well.

684 If CO_2 leaks through a fault or fracture, brine will start leaking before CO_2 (Rutqvist and
685 Tsang, 2002), which will induce a temperature increase along the fracture due to the warmer
686 temperature of the upwards flowing brine (Zeidouni et al., 2014). But the leaking CO_2, which
687 is in supercritical conditions at the storage formation from which CO_2 leaks, may change to
688 liquid conditions as it leaks upwards through a fault (Pruess, 2005a). Simulation results of
689 Pruess (2005a) show that liquid CO_2 boils into gas at around 630 m because at this depth the
690 pressure and temperature of CO_2 are such that they lie on the saturation line. The phase
691 change from liquid to gas is accompanied by a large increase in volume, i.e., a large density
692 decrease, and a decrease in viscosity. As a result of CO_2 depressurization and expansion as it
693 migrates towards shallower depths, temperature will decrease due to the Joule-Thomson
694 cooling effect. Furthermore, temperature will drop because latent heat is absorbed by the
695 phase change process. The region where CO_2 changes its phase from liquid to gas becomes a

696 3-phase region because there is water present (Pruess, 2005b). Mobility is significantly
697 reduced in this region, which hinders CO_2 upflow locally and promotes lateral spreading of
698 CO_2. The decrease in CO_2 flow causes the temperature to increase again due to heat
699 conduction from the surrounding rock, increasing the temperature and eventually recovering a
700 two-phase flow that allows upward CO_2 flow again. This leads to a quasi-periodic discharge
701 of CO_2 towards the surface that shows a tendency to increase its period with time. Pruess
702 (2005a) also performed a simulation in which temperature was artificially maintained constant
703 by specifying very large rock specific heat. A constant temperature led to a monotonic
704 increase of leakage fluxes with time, also observed in an isothermal numerical simulation
705 performed by Pruess and Garcia (2002), without the formation of the 3-phase region. This
706 difference allowed Pruess (2005a) to conclude that the availability of conductive heat transfer
707 is the limiting factor of the growth of CO_2 fluxes when non-isothermal effects are taken into
708 account.

709 Simulation results show that the strong dependency of the CO_2 properties on pressure and
710 temperature leads to complex processes that can have either positive or negative feedback on
711 the CO_2 leakage rates. The decrease in both CO_2 density and viscosity as CO_2 migrates
712 upwards provides a self-enhancement of the leakage rate. However, strong cooling caused by
713 phase change from liquid to gaseous CO_2 may cause three-phase flow that self-limits leakage
714 and may give rise to geysering (e.g., Pruess, 2008). Since thermal effects play a relevant role
715 in CO_2 leakage processes, measuring temperature along wells can be useful to detect leakage.

716 The temperature signal can be used to detect not only CO_2 leakage, but also brine leakage.
717 If brine leakage occurs, temperature will increase because of the warmer temperature of the
718 brine that comes from deeper depths. But if brine leakage is followed by CO_2 leakage, cooling
719 will take place once CO_2 reaches a certain depth due to CO_2 expansion. The main drawback
720 of leakage detection using temperature signals is that the leakage-induced temperature

changes cover a small volume around the leakage pathway, which makes it difficult to detect unless the monitoring well is very close to where leakage occurs (Tao et al., 2013). In contrast, the pressure signal extends rapidly over large distances, but increases regardless of the fluid that is leaking. Thus, a combination of pressure with temperature monitoring is recommendable, because pressure monitoring can detect pressure perturbations which origin is located far away from the measurement point and if the temperature measurements are close to leakage, information on the leaking fluid can be obtained (Hurter et al., 2007).

Underground temperature and pressure monitoring can be combined with deformation measurements to detect leakage because deformation spreads instantaneously in response to overpressure (Rutqvist, 2012). Surface uplift evolution can be measured with InSAR, as it was successfully done at In Salah, Algeria (Vasco et al., 2008). Even though deformation measurements do not directly inform about thermal effects, their interpretation using coupled thermo-hydro-mechanical numerical simulations may allow determining the extension of the cooled region around injection wells because the contraction of the rock induced by cooling reduces the magnitude of the surface uplift (Goodarzi et al., 2015).

Temperature can be monitored using point measurements, wireline-deployed instruments or fiber-optic distributed temperature sensing (DTS) cables (Reinsch et al., 2013; Nuñez-Lopez et al., 2014). The wireline-deployed instruments provide logs of temperature as a function of depth and the DTS produces continuous temperature measurements both in time and space along the cable. DTS can provide, after careful calibration, resolution and accuracy as small as 0.02 and 0.3 ºC, respectively, as reported for a gas-hydrate monitoring application at around 1,200 m deep (Henninges et al., 2005). Hoang et al. (2011) used DTS to infer the productive zones after hydraulic fracturing operations from temperature measurements outside of the well. Concerning geologic carbon storage, temperature measurements have

745 already been performed at CO_2 pilot test sites, like Frio, Texas (Hovorka et al., 2006) and
746 industrial scale sites, like Cranfield, Mississippi (Hovorka et al., 2013).
747
748 ## 7. RESEARCH GAPS AND CHALLENGES
749 Based on the review of thermal effects on geologic carbon storage, a series of research
750 gaps and challenges have been identified. The following list suggests future research lines to
751 address them:
752 - The effect of impurities on corrosion of pipelines needs to be better understood.
753 Pipeline corrosion may lead to the failure of pipelines and thus, it is crucial to develop
754 guidelines for the metal requirements of pipelines depending on the flue gas composition.
755 These guidelines should take into account the possibility of strong cooling caused by
756 expansion of CO_2 if normal operation is interrupted suddenly.
757 - The connection between CO_2 transport and injection into the well is still associated
758 with significant uncertainties. Huge amounts of energy can be saved, and even generated, by
759 employing smart ways of using the high pressure at which liquid CO_2 is transported through
760 pipelines.
761 - Wellbore and reservoir simulators are usually decoupled. However, the pressure and
762 temperature at the bottom of the injection well should coincide with those in the storage
763 formation at the injection well. Coupling these two simulators will permit obtaining realistic
764 injection conditions that could be used to optimize the pressure and temperature at the
765 wellhead.
766 - The thermo-mechanical effects of cold CO_2 injection have not been widely
767 investigated and are not fully understood. In particular, different studies on caprock stability
768 due to cooling give results that are not in full agreement. Thus, the processes that govern
769 caprock stability are still not well-known and further investigation is required.

- The effect of geochemical reactions (dissolution/precipitation) on the geomechanical properties and responses of different rock types has not been addressed in detail. The combined work of geochemist with geomechanical experts is required to shed light on this coupled effect.

- Coupled thermo-hydro-mechanical-chemical processes have not been investigated yet in detail due to the high complexity of this problem that involves extremely high computational cost. To address this coupled problem, more efficient numerical simulators are required.

- Further investigation is needed to understand three-phase (water, gaseous CO_2 and liquid CO_2) relative permeability and hysteresis. Three-phase may form in CO_2 leakage pathways and may lead to a self-limiting feedback that decreases the leakage rate. However, the capillary properties of three-phase flow are not well-known.

- The geomechanical implications of CO_2 leakage related to cooling effects, especially when liquid CO_2 is formed, have not been investigated yet.

- CCUS: one of the main barriers to put in practice CCS is its elevated cost. To reduce its cost, adding a "utilization" that provides an economic benefit is highly recommendable. More efforts should be devoted to develop CCUS options.

- Finally, to achieve a successful deployment of CCS and CCUS, there should be a transition from pilot to demonstration scale sites. The Boundary Dam Carbon Capture Project, in Saskatchewan, Canada, has been the first commercial-scale CCS project. This is a great first start, but it should be followed by many other industrial scale projects.

ACKNOWLEDGMENTS

V.V. acknowledges financial support from the "TRUST" project (European Community's Seventh Framework Programme FP7/2007-2013 under grant agreement n 309607) and from

“FracRisk" project (European Community's Horizon 2020 Framework Programme H2020-EU.3.3.2.3 under grant agreement n 640979). This work was funded in part by the Assistant Secretary for Fossil Energy, National Energy Technology Laboratory, National Risk Assessment Partnership, of the U.S. Department of Energy under Contract No. DEAC02-05CH11231.

REFERENCES

Adams, B. M., Kuehn, T. H., Bielicki, J. M., Randolph, J. B., & Saar, M. O. (2014). On the importance of the thermosiphon effect in CPG (CO_2 plume geothermal) power systems. *Energy*, *69*, 409-418.

Adams, B. M., Kuehn, T. H., Bielicki, J. M., Randolph, J. B., & Saar, M. O. (2015). A comparison of electric power output of CO_2 Plume Geothermal (CPG) and brine geothermal systems for varying reservoir conditions. *Applied Energy*, *140*, 365-377.

Alnes, H., Eiken, O., Nooner, S., Sasagawa, G., Stenvold, T., & Zumberge, M. (2011). Results from Sleipner gravity monitoring: updated density and temperature distribution of the CO_2 plume. *Energy Procedia*, *4*, 5504-5511.

André, L., Azaroual, M., Peysson, Y., & Bazin, B. (2011). Impact of porous medium desiccation during anhydrous CO_2 injection in deep saline aquifers: Up scaling from experimental results at laboratory scale to near-well region. *Energy Procedia*, *4*, 4442-4449.

André, L., Azaroual, M., & Menjoz, A. (2010). Numerical simulations of the thermal impact of supercritical CO_2 injection on chemical reactivity in a carbonate saline reservoir. *Transport in porous media*, *82*(1), 247-274.

818 Ardelan, M. V., & Steinnes, E. (2010). Changes in mobility and solubility of the redox
819 sensitive metals Fe, Mn and Co at the seawater-sediment interface following CO_2 seepage.
820 *Biogeosciences, 7*(2), 569-583.
821 Aspelund, A., Mølnvik, M. J., & De Koeijer, G. (2006). Ship Transport of CO_2: Technical
822 Solutions and Analysis of Costs, Energy Utilization, Exergy Efficiency and CO_2
823 Emissions. *Chemical Engineering Research and Design*, *84*(9), 847-855.
824 Bachu, S. (2003). Screening and ranking of sedimentary basins for sequestration of CO_2 in
825 geological media in response to climate change. *Environmental Geology, 44*(3), 277-289.
826 Bao, J., Xu, Z., & Fang, Y. (2014). A coupled thermal-hydro-mechanical simulation for
827 carbon dioxide sequestration. *Environmental Geotechnics*, doi: 10.1680/envgeo.14.00002.
828 Baxter, P. J., Baubron, J. C., & Coutinho, R. (1999). Health hazards and disaster potential of
829 ground gas emissions at Furnas volcano, Sao Miguel, Azores. *Journal of Volcanology and*
830 *Geothermal Research*, *92*(1), 95-106.
831 Bielinski, A., Kopp, A., Schütt, H., & Class, H. (2008). Monitoring of CO_2 plumes during
832 storage in geological formations using temperature signals: Numerical investigation.
833 *International Journal of Greenhouse Gas Control*, *2*(3), 319-328.
834 Birkholzer, J. T., Zhou, Q., & Tsang, C. F. (2009). Large-scale impact of CO_2 storage in deep
835 saline aquifers: a sensitivity study on pressure response in stratified systems. *International*
836 *Journal of Greenhouse Gas Control*, *3*(2), 181-194.
837 Bissell, R. C., Vasco, D. W., Atbi, M., Hamdani, M., Okwelegbe, M., & Goldwater, M. H.
838 (2011). A full field simulation of the In Salah gas production and CO 2 storage project
839 using a coupled geo-mechanical and thermal fluid flow simulator. *Energy Procedia*, *4*,
840 3290-3297.

841 Bonneville, A., Nguyen, B. N., Stewart, M., Hou, Z. J., Murray, C., & Gilmore, T. (2014).
842 Geomechanical evaluation of thermal impact of injected CO_2 temperature on a geological
843 reservoir: application to the FutureGen 2.0 Site. *Energy Procedia*, *63*, 3298-3304.
844 Böttcher, N., Taron, J., Kolditz, O., Park, C. H., & Liedl, R. (2012). Evaluation of thermal
845 equations of state for CO_2 in numerical simulations. *Environmental Earth Sciences*, *67*(2),
846 481-495.
847 Brill, J., Mukherjee, H., (1999). Multiphase Flow in Wells. Henry L. Doherty Memorial Fund
848 of AIME, Society of Petroleum Engineers Inc., Richardson, TX.
849 Brown, G., Carvalho, V., Wray, A., Smith, D., Toombs, M., & Pennell, S. (2004). Monitoring
850 alternating CO_2 and water injection and its effect on production in a carbonate reservoir
851 using permanent fiber-optic distributed temperature systems. In *SPE Annual Technical*
852 *Conference and Exhibition*, Houston, Texas, 26–29 September 2004.
853 Burnett, E. S. (1923). Experimental study of the Joule-Thomson effect in carbon dioxide.
854 *Physical Review*, *22*(6), 590.
855 Buscheck, T. A., Elliot, T. R., Celia, M. A., Chen, M., Sun, Y., Hao, Y., Lu, C., Wolery, T. J.
856 & Aines, R. D. (2013). Integrated geothermal-CO_2 reservoir systems: reducing carbon
857 intensity through sustainable energy production and secure CO_2 storage. *Energy Procedia*,
858 *37*, 6587-6594.
859 Celia, M. A., Bachu, S., Nordbotten, J. M., & Bandilla, K. W. (2015). Status of CO_2 storage
860 in deep saline aquifers with emphasis on modeling approaches and practical simulations.
861 *Water Resources Research*, *51*(9), 6846-6892.
862 Charnley, A., Rowlinson, J. S., Sutton, J. R., & Townley, J. R. (1955). The isothermal Joule-
863 Thomson coefficient of some binary gas mixtures. *Proceedings of the Royal Society of*
864 *London. Series A. Mathematical and Physical Sciences*, *230*(1182), 354-358.

865 Choi, I. H., Lee, S., Seo, Y., & Chang, D. (2013). Analysis and optimization of cascade
866 Rankine cycle for liquefied natural gas cold energy recovery. *Energy*, *61*, 179-195.
867 Class, H., Ebigbo, A., Helmig, R., Dahle, H. K., Nordbotten, J. M., Celia, M. A., Audigane,
868 P., Darcis, M., Ennis-King, J., Fan, Y., Flemisch, B., Gasda, S. E., Jin, M., Krug, S.,
869 Labregere, D., Beni, A. N., Pawar, R. J., Sbai, A., Thomas, S. G., Trenty, L., & Wei, L.
870 (2009). A benchmark study on problems related to CO_2 storage in geologic formations.
871 *Computational Geosciences*, *13*(4), 409-434.
872 de Simone, S., Vilarrasa, V., Carrera, J., Alcolea, A., & Meier, P. (2013). Thermal coupling
873 may control mechanical stability of geothermal reservoirs during cold water injection.
874 *Physics and Chemistry of the Earth, Parts A/B/C*, *64*, 117-126.
875 Ding, T., & Liu, Y. (2014). Simulations and analysis of hydrate formation during CO_2
876 injection into cold saline aquifers. *Energy Procedia*, *63*, 3030-3040.
877 Duan, Z., & Sun, R. (2003). An improved model calculating CO_2 solubility in pure water and
878 aqueous NaCl solutions from 273 to 533 K and from 0 to 2000 bar. *Chemical geology*,
879 *193*(3), 257-271.
880 Ebigbo, A., Class, H., & Helmig, R. (2007). CO_2 leakage through an abandoned well:
881 problem-oriented benchmarks. *Computational Geosciences*, *11*(2), 103-115.
882 Elliot, T. R., Buscheck, T. A., & Celia, M. (2013). Active CO_2 reservoir management for
883 sustainable geothermal energy extraction and reduced leakage. *Greenhouse Gases: Science*
884 *and Technology*, *3*(1), 50-65.
885 Eurostat (2016). Consumption of Energy. ec.europa.eu/eurostat/statistics-
886 explained/index.php/Consumption_of_energy. Consulted on July 25, 2016.
887 Fang, Y., Nguyen, B. N., Carroll, K., Xu, Z., Yabusaki, S. B., Scheibe, T. D., & Bonneville,
888 A. (2013). Development of a coupled thermo-hydro-mechanical model in discontinuous

media for carbon sequestration. *International Journal of Rock Mechanics and Mining Sciences*, *62*, 138-147.

Freifeld, B., Zakim, S., Pan, L., Cutright, B., Sheu, M., Doughty, C., & Held, T. (2013). Geothermal energy production coupled with CCS: a field demonstration at the SECARB Cranfield Site, Cranfield, Mississippi, USA. *Energy Procedia*, *37*, 6595-6603.

Gale, J., & Davison, J. (2004). Transmission of CO_2—safety and economic considerations. *Energy*, *29*(9), 1319-1328.

Gale, J., (2004). Geological storage of CO_2: What do we know, where are the gaps and what more needs to be done? *Energy 29*, 1329-1338.

Gasda, S. E., Bachu, S., & Celia, M. A. (2004). Spatial characterization of the location of potentially leaky wells penetrating a deep saline aquifer in a mature sedimentary basin. *Environmental geology*, *46*(6-7), 707-720.

Ghassemi, A., Tarasovs, S., & Cheng, A. D. (2007). A 3-D study of the effects of thermomechanical loads on fracture slip in enhanced geothermal reservoirs. *International Journal of Rock Mechanics and Mining Sciences*, *44*(8), 1132-1148.

Goodarzi, S., Settari, A., Zoback, M. D., & Keith, D. (2010). Thermal aspects of geomechanics and induced fracturing in CO_2 injection with application to CO_2 sequestration in Ohio River Valley. In *SPE International Conference on CO_2 Capture, Storage, and Utilization*. New Orleans, Louisiana, 10-12 November 2010.

Goodarzi, S., Settari, A., & Keith, D. (2011). Geomechanical modeling for CO_2 storage in Wabamun Lake Area of Alberta, Canada. *Energy Procedia*, *4*, 3399-3406.

Goodarzi, S., Settari, A., & Keith, D. (2012). Geomechanical modeling for CO_2 storage in Nisku aquifer in Wabamun Lake area in Canada. *International Journal of Greenhouse Gas Control*, *10*, 113-122.

913 Goodarzi, S., Settari, A., Zoback, M., & Keith, D. W. (2013). Thermal effects on shear
914 fracturing and injectivity during CO_2 storage. In *ISRM International Conference for*
915 *Effective and Sustainable Hydraulic Fracturing*, Brisbane, Australia, 20-22 May 2013.
916 Goodarzi, S., Settari, A., Zoback, M.D., & Keith, D.W. (2015). Optimization of a CO_2 storage
917 project based on thermal, geomechanical and induced fracturing effects. *Journal of*
918 *Petroleum Science and Engineering*, *134*, 49-59.
919 Gor, G. Y., Elliot, T. R., & Prévost, J. H. (2013). Effects of thermal stresses on caprock
920 integrity during CO_2 storage. *International Journal of Greenhouse Gas Control*, *12*, 300-
921 309.
922 Gor, G. Y., & Prévost, J. H. (2013). Effect of CO_2 Injection Temperature on Caprock
923 Stability. *Energy Procedia*, *37*, 3727-3732.
924 Han, W. S., Stillman, G. A., Lu, M., Lu, C., McPherson, B. J., & Park, E. (2010). Evaluation
925 of potential nonisothermal processes and heat transport during CO_2 sequestration. *Journal*
926 *of Geophysical Research: Solid Earth (1978–2012)*, *115*(B7).
927 Han, W. S., Kim, K. Y., Park, E., McPherson, B. J., Lee, S. Y., & Park, M. H. (2012).
928 Modeling of spatiotemporal thermal response to CO_2 injection in saline formations:
929 Interpretation for monitoring. *Transport in porous media*, *93*(3), 381-399.
930 Hansen, O., Gilding, D., Nazarian, B., Osdal, B., Ringrose, P., Kristoffersen, J. B., Eiken, O.
931 & Hansen, H. (2013). Snøhvit: the history of injecting and storing 1 Mt CO_2 in the Fluvial
932 Tubåen Fm. *Energy Procedia*, *37*, 3565-3573.
933 Harvey, A. H. (1996). Semiempirical correlation for Henry's constants over large temperature
934 ranges. *AIChE journal*, *42*(5), 1491-1494.
935 Henninges, J., Huenges, E., & Burkhardt, H. (2005). In situ thermal conductivity of
936 gas-hydrate-bearing sediments of the Mallik 5L-38 well. *Journal of Geophysical Research:*
937 *Solid Earth (1978–2012)*, *110*(B11).

938 Henninges, J., Liebscher, A., Bannach, A., Brandt, W., Hurter, S., Köhler, S., Möller, F. &
939 CO2SINK Group. (2011). PT-ρ and two-phase fluid conditions with inverted density
940 profile in observation wells at the CO_2 storage site at Ketzin (Germany). *Energy Procedia*,
941 *4*, 6085-6090.
942 Hepple, R. P., & Benson, S. M. (2005). Geologic storage of carbon dioxide as a climate
943 change mitigation strategy: performance requirements and the implications of surface
944 seepage. *Environmental Geology*, *47*(4), 576-585.
945 Hergert, T., Heidbach, O., Reiter, K., Giber, S.B. & Marschall, P. (2015). Stress field
946 sensitivity analysis in a sedimentary sequence of the Alpine foreland, northern
947 Switzerland. *Solid Earth*, *6*, 533-552.
948 Hill, B., Hovorka, S., & Melzer, S. (2013). Geologic carbon storage through enhanced oil
949 recovery. *Energy Procedia*, *37*, 6808-6830.
950 Hoang, H., Mahadevan, J., & Lopez, H. D. (2011). Interpretation of wellbore temperatures
951 measured using distributed temperature sensors during hydraulic fracturing. In *SPE*
952 *Hydraulic Fracturing Technology Conference*. Society of Petroleum Engineers.
953 Hovorka, S. D., Benson, S. M., Doughty, C., Freifeld, B. M., Sakurai, S., Daley, T. M.,
954 Kharaka, Y. K., Holtz, M. H., Trautz, R. C., Nance, H. S., Myer, L. R., & Knauss, K. G.
955 (2006). Measuring permanence of CO_2 storage in saline formations: the Frio experiment.
956 *Environmental Geosciences*, *13*(2), 105-121.
957 Hovorka, S. D., Meckel, T. A., & Treviño, R. H. (2013). Monitoring a large-volume injection
958 at Cranfield, Mississippi—project design and recommendations. *International Journal of*
959 *Greenhouse Gas Control*, *18*, 345-360.
960 Hurter, S., Garnett, A. A., Bielinski, A., & Kopp, A. (2007). Thermal signature of free-phase
961 CO_2 in porous rocks: detectability of CO_2 by temperature logging. *SPE Offshore Europe*,
962 SPE 109007, Aberdeen, Scotland, UK, 4-7 September.

963 IEAGHG (2013). CO_2 pipeline infrastructure. Report 2013/18.
964 IPCC (Intergovernmental Panel on Climate Change) (2005). In: Metz, B., Davidson, O., de
965 Coninck, H.C., Loos, M. & Mayer, L.A. (eds). Special report on carbon dioxide capture
966 and storage. Cambridge University Press, Cambridge.
967 Jackson, S. J., Stevens, D., Giddings, D., & Power, H. (2015). Dynamic-wetting effects in
968 finite-mobility-ratio Hele-Shaw flow. *Physical Review E*, *92*(2), 023021.
969 Jeanne, P., Rutqvist, J., Dobson, P. F., Walters, M., Hartline, C., & Garcia, J. (2014). The
970 impacts of mechanical stress transfers caused by hydromechanical and thermal processes
971 on fault stability during hydraulic stimulation in a deep geothermal reservoir. *International*
972 *Journal of Rock Mechanics and Mining Sciences*, *72*, 149-163.
973 Kaldal, G. S., Jónsson, M. Þ., Pálsson, H., & Karlsdóttir, S. N. (2015). Structural Analysis of
974 Casings in High Temperature Geothermal Wells in Iceland. *Proceedings of World*
975 *Geothermal Congress 2015*, Melboune, Australia, 19-25 April 2015.
976 Kervévan, C., Beddelem, M. H., & O'Neil, K. (2014). CO_2-DISSOLVED: a Novel Concept
977 Coupling Geological Storage of Dissolved CO_2 and Geothermal Heat Recovery–Part 1:
978 Assessment of the Integration of an Innovative Low-cost, Water-based CO_2 Capture
979 Technology. *Energy Procedia*, *63*, 4508-4518.
980 Kim, K. Y., Han, W. S., Oh, J., Kim, T., & Kim, J. C. (2012). Characteristics of salt-
981 precipitation and the associated pressure build-up during CO_2 storage in saline aquifers.
982 *Transport in porous media*, *92*(2), 397-418.
983 Kim, S., & Hosseini, S. A. (2014a). Above-zone pressure monitoring and geomechanical
984 analyses for a field-scale CO_2 injection project in Cranfield, MS. *Greenhouse Gases:*
985 *Science and Technology*, *4*(1), 81-98.

Kim, S., & Hosseini, S. A. (2014b). Geological CO_2 storage: Incorporation of pore-pressure/stress coupling and thermal effects to determine maximum sustainable pressure limit. *Energy Procedia*, *63*, 3339-3346.

Kim, S., & Hosseini, S. A. (2015). Hydro-thermo-mechanical analysis during injection of cold fluid into a geologic formation. *International Journal of Rock Mechanics and Mining Sciences*, *77*, 220-236.

Koschel, D., Coxam, J. Y., Rodier, L., & Majer, V. (2006). Enthalpy and solubility data of CO_2 in water and NaCl (aq) at conditions of interest for geological sequestration. *Fluid Phase Equilibria*, *247*(1), 107-120.

Krogh, E., Nilsen, R., & Henningsen, R. (2012). Liquefied CO_2 Injection Modelling. *Energy Procedia*, *23*, 527-555.

LaForce, T., Ennis-King, J., & Paterson, L. (2015). Semi-analytical temperature and stress profiles for nonisothermal CO_2 injection. In *Proceedings of the World Geothermal Congress*, Melbourne, Australia, 19-25 April 2015.

Le Quéré, C., Moriarty, R., Andrew, R. M., et al. (2015). Global carbon budget 2015. *Earth System Science Data*, *7*(2), 349-396.

Liebscher, A., Möller, F., Bannach, A., Köhler, S., Wiebach, J., Schmidt-Hattenberger, C., Weiner, M., Pretschner, C., Ebert, K., & Zemke, J. (2013). Injection operation and operational pressure–temperature monitoring at the CO_2 storage pilot site Ketzin, Germany—Design, results, recommendations. *International Journal of Greenhouse Gas Control*, *15*, 163-173.

Lindeberg, E. (2011). Modelling pressure and temperature profile in a CO2 injection well. *Energy Procedia*, *4*, 3935-3941.

1009 Lu, J., Partin, J. W., Hovorka, S. D., & Wong, C. (2010). Potential risks to freshwater
1010 resources as a result of leakage from CO_2 geological storage: a batch-reaction experiment.
1011 *Environmental Earth Sciences*, *60*(2), 335-348.
1012 Lu, M., & Connell, L. D. (2008). Non-isothermal flow of carbon dioxide in injection wells
1013 during geological storage. *International journal of greenhouse gas control*, *2*(2), 248-258.
1014 Lu, M., & Connell, L. D. (2014a). Transient, thermal wellbore flow of multispecies carbon
1015 dioxide mixtures with phase transition during geological storage. *International Journal of*
1016 *Multiphase Flow*, *63*, 82-92.
1017 Lu, M., & Connell, L. D. (2014b). The transient behaviour of CO_2 flow with phase transition
1018 in injection wells during geological storage–Application to a case study. *Journal of*
1019 *Petroleum Science and Engineering*, *124*, 7-18.
1020 Luo, Z., & Bryant, S. L. (2010). Influence of thermo-elastic stress on CO_2 injection induced
1021 fractures during storage. In *SPE International Conference on CO_2 capture, storage, and*
1022 *utilization*, New Orleans, Louisiana, 10-12 November 2010.
1023 Luo, Z., & Bryant, S. (2011). Influence of thermo-elastic stress on fracture initiation during
1024 CO_2 injection and storage. *Energy Procedia*, *4*, 3714-3721.
1025 Luo, Z., Bryant, S., & Meckel, T. (2013). Application of improved injection well temperature
1026 model to Cranfield measurements. *Energy Procedia*, *37*, 4128-4135.
1027 Luo, Z., & Bryant, S. (2013). Can we Overcome Thermo-elastic Limits on CO_2 Injection
1028 Rates in Horizontal Wells?. *Energy Procedia*, *37*, 3299-3306.
1029 Luo, Z., & Bryant, S. (2014). Impacts of injection induced fractures propagation in CO_2
1030 geological sequestration–is fracturing good or bad for CO_2 sequestration. *Energy Procedia*,
1031 *63*, 5394-5407.

1032 Mathias, S. A., Gluyas, J. G., Oldenburg, C. M., & Tsang, C. F. (2010). Analytical solution
1033 for Joule–Thomson cooling during CO_2 geo-sequestration in depleted oil and gas
1034 reservoirs. *International Journal of Greenhouse Gas Control*, *4*(5), 806-810.
1035 Mathias, S. A., Gluyas, J. G., González Martínez de Miguel, G. J., & Hosseini, S. A. (2011).
1036 Role of partial miscibility on pressure buildup due to constant rate injection of CO_2 into
1037 closed and open brine aquifers. *Water Resources Research*, *47*(12), W12525.
1038 Matter, J. M., Stute, M., Snæbjörnsdottir, S. Ó., Oelkers, E. H., Gislason, S. R., Aradottir, E.
1039 S., ... & Axelsson, G. (2016). Rapid carbon mineralization for permanent disposal of
1040 anthropogenic carbon dioxide emissions. *Science*, *352*(6291), 1312-1314.
1041 McCoy, S. T., & Rubin, E. S. (2008). An engineering-economic model of pipeline transport
1042 of CO_2 with application to carbon capture and storage. *International Journal of*
1043 *Greenhouse Gas Control*, *2*(2), 219-229.
1044 McCulloch, J., Gastineau, J., Bour, D. L., & Ravi, K. (2003). Life cycle modeling of wellbore
1045 cement used for enhanced geothermal system development. *Geothermal Resources*
1046 *Council Transactions*, *27*, 147-154.
1047 McPherson, B. J., Han, W. S., & Cole, B. S. (2008). Two equations of state assembled for
1048 basic analysis of multiphase CO_2 flow and in deep sedimentary basin conditions.
1049 *Computers & Geosciences*, *34*(5), 427-444.
1050 Miocic, J. M., Gilfillan, S., McDermott, C., & Haszeldine, R. S. (2013). Mechanisms for CO_2
1051 Leakage Prevention–A Global Dataset of Natural Analogues. *Energy Procedia*, *40*, 320-
1052 328.
1053 Möller, F., Liebscher, A., Martens, S., Schmidt-Hattenberger, C., & Streibel, M. (2014).
1054 Injection of CO_2 at ambient temperature conditions–pressure and temperature results of the
1055 “cold injection” experiment at the Ketzin pilot site. *Energy Procedia*, *63*, 6289-6297.

1056 Munkejord, S. T., Jakobsen, J. P., Austegard, A., & Mølnvik, M. J. (2010). Thermo-and fluid-
1057 dynamical modelling of two-phase multi-component carbon dioxide mixtures.
1058 *International Journal of Greenhouse Gas Control*, *4*(4), 589-596.
1059 Nimtz, M., Klatt, M., Wiese, B., Kühn, M., & Joachim Krautz, H. (2010). Modelling of the
1060 CO_2 process-and transport chain in CCS systems—Examination of transport and storage
1061 processes. *Chemie der Erde-Geochemistry*, *70*, 185-192.
1062 Nooner, S. L., Eiken, O., Hermanrud, C., Sasagawa, G. S., Stenvold, T., & Zumberge, M. A.
1063 (2007). Constraints on the in situ density of CO_2 within the Utsira formation from time-
1064 lapse seafloor gravity measurements. *International Journal of Greenhouse Gas Control*,
1065 *1*(2), 198-214.
1066 Nordbotten, J. M., Celia, M. A., & Bachu, S. (2004). Analytical solutions for leakage rates
1067 through abandoned wells. *Water Resources Research*, *40*(4).
1068 Nordbotten, J. M., Celia, M. A., Bachu, S., & Dahle, H. K. (2005). Semianalytical solution for
1069 CO2 leakage through an abandoned well. *Environmental science & technology*, *39*(2), 602-
1070 611.
1071 Nuñez-Lopez, V., Muñoz-Torres, J., & Zeidouni, M. (2014). Temperature monitoring using
1072 Distributed Temperature Sensing (DTS) technology. *Energy Procedia*, *63*, 3984-3991.
1073 Ochsner, K. (2008). Carbon dioxide heat pipe in conjunction with a ground source heat pump
1074 (GSHP). *Applied Thermal Engineering*, *28*(16), 2077-2082.
1075 Oldenburg, C. M. (2007). Joule-Thomson cooling due to CO_2 injection into natural gas
1076 reservoirs. *Energy Conversion and Management*, *48*(6), 1808-1815.
1077 Oldenburg, C. M., Doughty, C., Peters, C. A., & Dobson, P. F. (2012). Simulations of
1078 long-column flow experiments related to geologic carbon sequestration: effects of outer
1079 wall boundary condition on upward flow and formation of liquid CO_2. *Greenhouse Gases:*
1080 *Science and Technology*, *2*(4), 279-303.

Osselin, F., Fen-Chong, T., Fabbri, A., Lassin, A., Pereira, J. M., & Dangla, P. (2013). Dependence on injection temperature and on aquifer's petrophysical properties of the local stress applying on the pore wall of a crystallized pore in the context of CO2 storage in deep saline aquifers. *The European Physical Journal Applied Physics*, *64*(02), 21101.

Pan, L., Oldenburg, C. M., Wu, Y. S., & Pruess, K. (2009). Wellbore flow model for carbon dioxide and brine. *Energy Procedia*, *1*(1), 71-78.

Pan, L., Oldenburg, C. M., Pruess, K., & Wu, Y. S. (2011). Transient CO_2 leakage and injection in wellbore-reservoir systems for geologic carbon sequestration. *Greenhouse Gases: Science and Technology*, *1*(4), 335-350.

Pan, L., & Oldenburg, C. M. (2014). T2Well—an integrated wellbore–reservoir simulator. *Computers & Geosciences*, *65*, 46-55.

Pan, L., Freifeld, B., Doughty, C., Zakem, S., Sheu, M., Cutright, B., & Terrall, T. (2015). Fully coupled wellbore-reservoir modeling of geothermal heat extraction using CO_2 as the working fluid. *Geothermics*, *53*, 100-113.

Paterson, L., Lu, M., Connell, L., & Ennis-King, J. P. (2008). Numerical modeling of pressure and temperature profiles including phase transitions in carbon dioxide wells. In *SPE Annual Technical Conference and Exhibition*. Society of Petroleum Engineers.

Paterson, L., Ennis-King, J. P., & Sharma, S. (2010). Observations of thermal and pressure transients in carbon dioxide wells. In *SPE Annual Technical Conference and Exhibition*. Society of Petroleum Engineers.

Pekot, L. J., Petit, P., Adushita, Y., Saunier, S., & De Silva, R. L. (2011). Simulation of two-phase flow in carbon dioxide injection wells. *Offshore Europe*, SPE-144847-MS, 6-8 September, Aberdeen, UK.

Pool, M., Carrera, J., Vilarrasa, V., Silva, O., & Ayora, C. (2013). Dynamics and design of systems for geological storage of dissolved CO_2. *Advances in Water Resources*, *62*, 533-542.

Preisig, M., & Prévost, J. H. (2011). Coupled multi-phase thermo-poromechanical effects. Case study: CO_2 injection at In Salah, Algeria. *International Journal of Greenhouse Gas Control*, *5*(4), 1055-1064.

Pruess, K., & Garcia, J. (2002). Multiphase flow dynamics during CO_2 disposal into saline aquifers. *Environmental Geology*, *42*(2-3), 282-295.

Pruess, K. (2005a). Numerical studies of fluid leakage from a geologic disposal reservoir for CO_2 show self-limiting feedback between fluid flow and heat transfer. *Geophysical research letters*, *32*(14).

Pruess, K. (2005b). Numerical simulations show potential for strong nonisothermal effects during fluid leakage from a geologic disposal reservoir for CO_2. *Dynamics of Fluids and Transport in Fractured Rock*, 81-89.

Pruess, K. (2008). On CO_2 fluid flow and heat transfer behavior in the subsurface, following leakage from a geologic storage reservoir. *Environmental Geology*, *54*(8), 1677-1686.

Pruess, K. (2011). Integrated modeling of CO_2 storage and leakage scenarios including transitions between super-and subcritical conditions, and phase change between liquid and gaseous CO_2. *Greenhouse Gases: Science and Technology*, *1*(3), 237-247.

Randolph, J. B., & Saar, M. O. (2011a). Combining geothermal energy capture with geologic carbon dioxide sequestration. *Geophysical Research Letters*, *38*(10).

Randolph, J. B., & Saar, M. O. (2011b). Coupling carbon dioxide sequestration with geothermal energy capture in naturally permeable, porous geologic formations: Implications for CO_2 sequestration. *Energy Procedia*, *4*, 2206-2213.

1128 Randolph, J. B., Saar, M. O., & Bielicki, J. (2013). Geothermal energy production at geologic
1129 CO_2 sequestration sites: impact of thermal drawdown on reservoir pressure. *Energy*
1130 *Procedia*, *37*, 6625-6635.
1131 Rayward-Smith, W. J., & Woods, A. W. (2011). Some implications of cold CO_2 injection into
1132 deep saline aquifers. *Geophysical Research Letters*, *38*(6).
1133 Redlich, O., & Kwong, J. N. (1949). On the thermodynamics of solutions. V. An equation of
1134 state. Fugacities of gaseous solutions. *Chemical reviews*, *44*(1), 233-244.
1135 Reinsch, T., Henninges, J., & Ásmundsson, R. (2013). Thermal, mechanical and chemical
1136 influences on the performance of optical fibres for distributed temperature sensing in a hot
1137 geothermal well. *Environmental Earth Sciences*, *70*(8), 3465-3480.
1138 Réveillère, A., & Rohmer, J. (2011). Managing the risk of CO_2 leakage from deep saline
1139 aquifer reservoirs through the creation of a hydraulic barrier. *Energy Procedia*, *4*, 3187-
1140 3194.
1141 Réveillère, A., Rohmer, J., & Manceau, J. C. (2012). Hydraulic barrier design and
1142 applicability for managing the risk of CO_2 leakage from deep saline aquifers. *International*
1143 *Journal of Greenhouse Gas Control*, *9*, 62-71.
1144 Roy, P., Walsh, S. D., Morris, J. P., Iyer, J., Hao, Y., Carroll, S., Gawell, K., Todorovic, J., &
1145 Torsæter, M. (2016). Studying the Impact of Thermal Cycling on Wellbore Integrity
1146 during CO_2 Injection. *Proceedings of the American Rock Mechanics Association*, paper 16-
1147 0668, Houston, Texas, 26-29 June, 2016.
1148 Rutqvist, J., & Tsang, C. F. (2002). A study of caprock hydromechanical changes associated
1149 with CO_2-injection into a brine formation. *Environmental Geology*, *42*(2-3), 296-305.
1150 Rutqvist, J., Liu, H. H., Vasco, D. W., Pan, L., Kappler, K., & Majer, E. (2011). Coupled non-
1151 isothermal, multiphase fluid flow, and geomechanical modeling of ground surface

deformations and potential for induced micro-seismicity at the In Salah CO_2 storage operation. *Energy Procedia*, *4*, 3542-3549.

Rutqvist, J. (2012). The geomechanics of CO_2 storage in deep sedimentary formations. *Geotechnical and Geological Engineering*, *30*(3), 525-551.

Saaltink, M. W., Vilarrasa, V., De Gaspari, F., Silva, O., Carrera, J., & Rötting, T. S. (2013). A method for incorporating equilibrium chemical reactions into multiphase flow models for CO_2 storage. *Advances in Water Resources*, *62*, 431-441.

Sagu, O. L., & Pao, W. K. (2013). In-situ stress perturbation due to temperature around borehole during carbon injection. *Asian Journal of Applied Sciences*, *6*(1), 40-49.

Sasaki, K., Yasunami, T., & Sugaia, Y. (2009). Prediction model of bottom hole temperature and pressure at deep injector for CO_2 sequestration to recover injection rate. *Energy Procedia*, *1*(1), 2999-3006.

Sato, K., Mito, S., Horie, T., Ohkuma, H., Saito, H., Watanabe, J., & Yoshimura, T. (2009). A monitoring framework for assessing underground migration and containment of carbon dioxide sequestered in an onshore aquifer. *Energy Procedia*, *1*(1), 2261-2268.

Shi, X., & Che, D. (2009). A combined power cycle utilizing low-temperature waste heat and LNG cold energy. *Energy conversion and management*, *50*(3), 567-575.

Silva, O., Carrera, J., & Vilarrasa, V. (2011). An efficient injection concept for the geological storage of CO_2. *6^{th} Trondheim CCS Conference*, Trondheim, Norway, 14-16 June 2011.

Singh, A. K., Goerke, U. J., & Kolditz, O. (2011a). Numerical simulation of non-isothermal compositional gas flow: application to carbon dioxide injection into gas reservoirs. *Energy*, *36*(5), 3446-3458.

Singh, A. K., Böttcher, N., Wang, W., Park, C. H., Görke, U. J., & Kolditz, O. (2011b). Non-isothermal effects on two-phase flow in porous medium: CO_2 disposal into a saline aquifer. *Energy Procedia*, *4*, 3889-3895.

Singh, A. K., Baumann, G., Henninges, J., Görke, U. J., & Kolditz, O. (2012). Numerical analysis of thermal effects during carbon dioxide injection with enhanced gas recovery: a theoretical case study for the Altmark gas field. *Environmental Earth Sciences*, *67*(2), 497-509.

Skinner, L. (2003). CO_2 blowouts: An emerging problem. *World Oil*, *224*(1), 38-42.

Skovholt, O. (1993). CO_2 transportation system. *Energy Conversion and Management*, *34*(9), 1095-1103.

Song, J., & Zhang, D. (2012). Comprehensive review of caprock-sealing mechanisms for geologic carbon sequestration. *Environmental science & technology*, *47*(1), 9-22.

Span, R., & Wagner, W. (1996). A new equation of state for carbon dioxide covering the fluid region from the triple- point temperature to 1100 K at pressures up to 800 MPa. *Journal of physical and chemical reference data*, *25*(6), 1509-1596.

Spycher, N., Pruess, K., & Ennis-King, J. (2003). CO_2-H_2O mixtures in the geological sequestration of CO_2. I. Assessment and calculation of mutual solubilities from 12 to 100° C and up to 600 bar. *Geochimica et Cosmochimica Acta*, *67*(16), 3015-3031.

Spycher, N., & Pruess, K. (2005). CO_2-H_2O mixtures in the geological sequestration of CO_2. II. Partitioning in chloride brines at 12–100° C and up to 600 bar. *Geochimica et Cosmochimica Acta*, *69*(13), 3309-3320.

Svensson, R., Odenberger, M., Johnsson, F., & StrÖmberg, L. (2004). Transportation systems for CO_2—application to carbon capture and storage. *Energy Conversion and Management*, *45*(15), 2343-2353.

Tao, Q., Bryant, S. L., & Meckel, T. A. (2013). Modeling above-zone measurements of pressure and temperature for monitoring CCS sites. *International Journal of Greenhouse Gas Control*, *18*, 523-530.

1201 Taylor, J., & Bryant, S. (2014). Quantifying thermally driven fracture geometry during CO_2
1202 storage. *Energy Procedia*, *63*, 3390-3404.
1203 Teodoriu, C. (2015). Why and When Does Casing Fail in Geothermal Wells: a Surprising
1204 Question?. *Proceedings of World Geothermal Congress 2015*, Melboune, Australia, 19-25
1205 April 2015.
1206 Tillner, E., Kempka, T., Nakaten, B., & Kühn, M. (2013). Brine migration through fault
1207 zones: 3D numerical simulations for a prospective CO_2 storage site in Northeast Germany.
1208 *International Journal of Greenhouse Gas Control*, *19*, 689-703.
1209 Trautz, R. C., Pugh, J. D., Varadharajan, C., Zheng, L., Bianchi, M., Nico, P. S., Spycher, N.
1210 F., Newell, D. L., Esposito, R. A., Wu, Y., Dafflon, B., Hubbard, S. S., & Birkholzer, J. T.
1211 (2012). Effect of dissolved CO_2 on a shallow groundwater system: A controlled release
1212 field experiment. *Environmental Science & Technology*, *47*(1), 298-305.
1213 Tutolo, B. M., Kong, X. Z., Seyfried, W. E., & Saar, M. O. (2015). High performance reactive
1214 transport simulations examining the effects of thermal, hydraulic, and chemical (THC)
1215 gradients on fluid injectivity at carbonate CCUS reservoir scales. *International Journal of*
1216 *Greenhouse Gas Control*, *39*, 285-301.
1217 Vasco, D. W., Ferretti, A. & Novali, F. (2008). Reservoir monitoring and characterization
1218 using satellite geodetic data: interferometric synthetic aperture radar observations from the
1219 Krechba field, Algeria. *Geophysics*, *73*(6), WA113–WA122.
1220 Verdon, J. P., Kendall, J. M., White, D. J., & Angus, D. A. (2011). Linking microseismic
1221 event observations with geomechanical models to minimise the risks of storing CO_2 in
1222 geological formations. *Earth and Planetary Science Letters*, *305*(1), 143-152.
1223 Vilarrasa, V., Silva, O., Carrera, J., & Olivella, S. (2013). Liquid CO_2 injection for geological
1224 storage in deep saline aquifers. *International Journal of Greenhouse Gas Control*, *14*, 84-
1225 96.

1226 Vilarrasa, V., Olivella, S., Carrera, J., & Rutqvist, J. (2014). Long term impacts of cold CO_2
1227 injection on the caprock integrity. *International Journal of Greenhouse Gas Control*, *24*, 1-
1228 13.
1229 Vilarrasa, V., Rutqvist, J., & Rinaldi, A. P. (2015). Thermal and capillary effects on the
1230 caprock mechanical stability at In Salah, Algeria. *Greenhouse Gases: Science and*
1231 *Technology*, *5*, 449-461.
1232 Vilarrasa, V., & Carrera, J. (2015). Geologic carbon storage is unlikely to trigger large
1233 earthquakes and reactivate faults through which CO2 could leak. *Proceedings of the*
1234 *National Academy of Sciences*, *112*(19), 5938-5943.
1235 Vilarrasa, V., & Laloui, L. (2015). Potential fracture propagation into the caprock induced by
1236 cold injection in normal faulting stress regimes. *Geomechanics for Energy and the*
1237 *Environment*, *2*, 22-31.
1238 Vilarrasa, V., & Laloui, L. (2016). Impacts of thermally induced stresses on fracture stability
1239 during geological storage of CO_2. *Energy Procedia*, *86*, 411-419.
1240 Vilarrasa, V. (2016). The role of the stress regime on microseismicity induced by
1241 overpressure and cooling in geologic carbon storage. *Geofluids*, doi: 10.1111/gfl.12197
1242 Wang, H., Shi, X., & Che, D. (2013). Thermodynamic optimization of the operating
1243 parameters for a combined power cycle utilizing low-temperature waste heat and LNG
1244 cold energy. *Applied Thermal Engineering*, *59*(1), 490-497.
1245 White, C.M., Smith, D.H., Jones, K.L., Goodman, A.L., Jikich, S.A., LaCount, R.B., DuBose,
1246 S.B., Ozdemir, E., Morsi, B.I., & Schroeder, K.T., (2005). Sequestration of carbon dioxide
1247 in coal with enhanced coalbed methane recovery a review. *Energy & Fuels 19*, 659-724.
1248 White, J.A., Chiaramonte, L., Ezzedine, S., Foxall, W., Hao, Y., Ramirez, A., & McNab, W.
1249 (2014). Geomechanical behaviour of the reservoir and caprock system at the In Salah CO2
1250 storage project. Proceedings of the National Academy of Sciences, *111*, 8747–8752.

1251 Wiese, B., Nimtz, M., Klatt, M., & Kühn, M. (2010). Sensitivities of injection rates for single
1252 well CO_2 injection into saline aquifers. *Chemie der Erde-Geochemistry*, *70*, 165-172.
1253 Wu, Y., & Bryant, S. L. (2014). Optimization of field-scale surface dissolution with
1254 thermoelastic constraints. *Energy Procedia*, *63*, 4850-4860.
1255 You, H., Seo, Y., Huh, C., & Chang, D. (2014). Performance analysis of cold energy recovery
1256 from CO_2 injection in ship-based Carbon Capture and Storage (CCS). *Energies*, *7*(11),
1257 7266-7281.
1258 Zeidouni, M., Nicot, J. P., & Hovorka, S. D. (2014). Monitoring above-zone temperature
1259 variations associated with CO_2 and brine leakage from a storage aquifer. *Environmental*
1260 *Earth Sciences*, 72:1733–1747.
1261 Zevenhoven, R., Fagerlund, J., & Songok, J. K. (2011). CO_2 mineral sequestration:
1262 developments toward large- scale application. *Greenhouse Gases: Science and*
1263 *Technology*, *1*(1), 48-57.
1264 Zhang, W., Li, Y., Xu, T., Cheng, H., Zheng, Y., & Xiong, P. (2009). Long-term variations of
1265 CO_2 trapped in different mechanisms in deep saline formations: a case study of the
1266 Songliao Basin, China. *International journal of greenhouse gas control*, *3*(2), 161-180.
1267 Zhang, Z. X., Wang, G. X., Massarotto, P., & Rudolph, V. (2006). Optimization of pipeline
1268 transport for CO_2 sequestration. *Energy Conversion and Management*, *47*(6), 702-715.
1269 Zhao, R., & Cheng, J. (2015). Non-isothermal modeling of CO_2 injection into saline aquifers
1270 at a low temperature. *Environmental Earth Sciences*, *73*(9), 5307-5316.
1271